Photocatalytic processes for the abatement of N-containing pollutants from waste water. Part 1: Inorganic pollutants

Matteo Compagnoni[a], Gianguido Ramis[b], Francesca S. Freyria[c], Marco Armandi[d], Barbara Bonelli[d], Ilenia Rossetti[a,*]

[a] *Dip. Chimica, Università degli Studi di Milano, CNR-ISTM and INSTM Unit Milano-Università, via C. Golgi 19, 20133 Milan, Italy*

[b] *Dip. Ing. Chimica, Civile ed Ambientale, Università degli Studi di Genova and INSTM Unit Genova, P.le Kennedy 1, 16129 Genoa, Italy*

[c]*Department of Chemistry, Massachusetts Institute of Technology, 77 Massachusetts Ave, 02139 Cambridge, MA, USA.*

[d]*Department of Applied Science and Technology and INSTM Unit of Torino-Politecnico, Politecnico di Torino, Corso Duca degli Abruzzi, 24, I-10129 Turin, Italy.*

Abstract

The development of effective methods for the abatement of some harmful pollutants from waste waters and from hydric resources is a challenging task. Nitrogen containing compounds, such as inorganic ammonia, nitrites and nitrates are harmful contaminants for drinking water, inducing acute and/or chronic diseases, especially affecting infants and children. Furthermore, when released in waste waters they contribute to eutrophication, or possibly contaminate ground water. This is particularly relevant in agriculturally intensive zones and in the case of some relevant industrial processes involving *e.g.* nitration reactions.

* Corresponding author: Fax: +390250314300; email ilenia.rossetti@unimi.it.

In the present paper, we review existing or innovative processes, mainly based on photocatalytic steps for the abatement of inorganic N-containing compounds from waste waters and for drinking water treatment, focusing on selectivity towards innocuous N_2.

Keywords: Nitrite; Nitrate; Ammonia; Photocatalytic abatement; Water treatment; Water pollution; Waste water; Drinking water; Water depuration; Semiconductor; Titania; Photocatalysis.

1 – Introduction

The World Health Organisation (WHO) introduced standard maximum and recommended levels of nitrates, nitrite and ammonium concentration in drinking water to be 50 ppm nitrate, 3 ppm nitrite and 0.5 ppm ammonium. Additionally, the Environment Protection Agency, US-EPA has set a drinking water maximum contaminant limit (MCL) for nitrate of 10 mg-N/L. A survey of 5101 wells in the US States revealed that nitrate levels exceed the standard in approximately 8% of wells with potential effect on 24.6 million people [1]. This makes nitrate the most ubiquitous contaminant found in drinking water sources [2].

Aqueous ammonia, one of the major nitrogen-containing pollutants in wastewater, is a potential source of oxygen depletion due to eutrophication [3]. Both ammonium and ammonia can be present in water and wastewater. There are several methods for NH_4^+/NH_3 removal, including biological nitrification, ammonia stripping, breakpoint chlorination and ion exchange, but each of these methods has disadvantages. For example, the efficiency of biological treatment is highly dependent on temperature, dissolved oxygen, the carbon source, pH, and the concentrations of toxic substances [4].

In nature, the nitrite ion is usually formed by ammonia oxidation through bacteria. It is often formed as a relatively stable intermediate during nitrate ion reduction. NO_2^- can react with secondary amines to produce nitrosoamines, which are carcinogens and may cause hypertension. Nitrites are also present in high concentration in caustic radioactive waste from nuclear plants, they are used as preservatives for food and are product of partial oxidation of N-containing compounds.

Environmental limits are defined by 'planetary boundaries'. The nitrogen cycle has already disrupted the safe operating limits, well beyond the criticisms brought about by climate change. Initial estimates suggest the ecosystem impacts of nitrogen pollution cost the EU-27 between €25 billion and €115 billion per year, and total costs (including those from N-related health and climate change impacts) could amount to €320 billion a year.

"A Blueprint to Safeguard Europe's Water Resources" has been published in Nov. 2012, highlighting that diffuse and point-source pollution are still significant problems for the water environment in about 38% and 22% of EU water bodies, respectively. Eutrophication due to excessive nutrient load remains a major threat to the good status of waters as nutrient enrichment is found in about 30% of water bodies in 17 Member States.

As a whole, ammonia, nitrites and nitrates are very common pollutants, especially produced in agricultural intensive zones and present in some specific industrial waste waters. Their effects are well recognised. For instance, nitrates can cause cyanosis in vulnerable individuals, especially infants and children (blue baby syndrome), by oxidation of Fe^{2+} to Fe^{3+} in hemoglobin centers, leading to species unable to transport oxygen (methemoglobin). Exposure to high levels of nitrates or nitrites has been also associated with increased incidence of cancer in adults, possible increased incidence of brain tumours, leukemia, and nasopharyngeal tumours in children [5, 6]. Other health effects following foetal exposure to elevated levels of nitrates in drinking water include intrauterine growth retardation [7],

increased incidence of Sudden Infant Death Syndrome (SIDS) [8], cardiac defects [9] and increased risk of nervous system defects [10].

As for ammonia in water, the US-EPA developed very recent regulations (2013) to update environmental and health protection against ammonia [11]. Ammonia comes from the metabolism of proteins and from ammonia containing fertilisers. It is toxic for invertebrates and fishes. The toxicity is commonly attributed only to NH_3, not to NH_4^+, but the equilibrium repartition of the two species in water depends on pH, temperature and ionic strength. In natural waters, the pH favours the ammonium ions as the predominant form at equilibrium. However, in alkaline waters, NH_3 can reach toxic levels (toxicity to aquatic organisms is only 20 μg/L). Its overall effects on human health for low exposure levels seem less relevant than those of nitrites and nitrates [12], although its eutrophication potential, as well as its capability to change pH of water is much more relevant.

Additionally, nitrites, nitrates and ammonium are well known nutrients and may lead to extensive eutrophication, if released in aqueous basins characterised by slow recirculation and exchange, such as lakes or closed basins. This phenomenon is due to the uncontrolled growth of phytoplankton and algae, caused by the increased nutrients feed, which leads to the depletion of oxygen and light for other species. This overpopulation of algae then brings to their death and uncontrolled release in water.

Biological treatments are standardised processes allowing the abatement of biodegradable organics from waste waters to meet common regulations. However, the legislative limits for N containing compounds can hardly be met by this standardised treatment, imposing further processes for N removal with additional costs.

Ion exchange traditionally has been used to remove nitrates from drinking water sources, but this process leaves behind a highly concentrated brine solution that still requires treatment. Alternatively, reverse osmosis and electro-dialysis may be used, which however

are expensive processes due to both installation and operating costs. Several methods have been developed and applied to the treatment of ammonia-containing wastewater, including biological processes, air stripping, ion exchange, breakpoint chlorination and chemical oxidation. Among these methods, biological processes are generally regarded to be the most efficient. However, they present disadvantages, including handling difficulties and large equipment requirements. Moreover, they are difficult to apply to treatment of wastewater that contains harmful co-existing species for bacteria.

Therefore, the development of cheaper and easily scalable systems for their abatement is more than welcome. Catalytic, electrocatalytic and photocatalytic processes are investigated for the reduction of NO_3^- and NO_2^- but the main issue still remains process selectivity, since over-reduction to NH_3/NH_4^+ is usually observed. For instance, catalytic hydrogenation over noble/base metals combinations, usually based on Pd, show some promise in terms of rates of nitrate removal, but it is usually limited in terms of the selectivity required to avoid undesired nitrite and ammonium formation.

This work summarises the main findings in the photocatalytic abatement of inorganic N-containing pollutants, which is a less explored research field with respect to other well explored photocatalytic processes.

2 – Catalytic reduction and photoreduction of nitrite and nitrate

The catalytic reduction of nitrate (Table 1) has been investigated by many authors [13, 14], according to this reaction scheme:

$NO_3^- + H_2 \rightarrow NO_2^- + H_2O$ 1)

$2\ NO_2^- + 3\ H_2 \rightarrow N_2 + 2\ H_2O + 2\ OH^-$ 2)

$NO_2^- + 3\ H_2 \rightarrow NH_4^+ + 2\ OH^-$ 3)
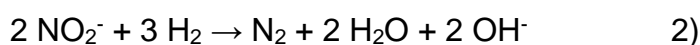
The reaction is usually carried out at moderate temperature, often 25°C, in semi-batch configuration by flowing hydrogen in continuous mode through the solution. Unfortunately, selectivity to innocuous N_2 is unsatisfactory in most cases, due to considerable formation of nitrite and ammonium through consecutive reactions. Noble metal based catalysts showed the best performance, usually promoted by a second metal component, such as Cu or Sn [15–17]. Nitrate was very rapidly converted, with accumulation of nitrite during the first minutes of reaction. Nitrite conversion was much slower, likely due to the accumulation of OH^-, which instead favoured ammonia formation [14]. When reducible supports such as TiO_2 are used, oxygen vacancies are formed by reduction in presence of H_2. Thus, nitrates adsorption can be favoured over vacancies. In the case of bimetallic Cu-Pd catalysts, nitrates are reduced over Cu, which oxidises to Cu^{2+} and is then reduced back to the metallic state thanks to H species formed by spillover on Pd particles. By contrast, Pd sites are considered responsible of the over-reduction of nitrite to ammonia.

Table 1: Examples of Catalytic reduction of NO_x^-.

Catalyst	Co-catalyst	Conversion NO_3^-, NO_2^- (%)	Selectivity N_2 (%)	Reference
TiO_2	Pd, Cu	95	56	14
Active C	Pd, Cu	100	80	16
$CuMgAlO_x$	Pt, Cu	30-80	90-50	17

The first pioneering studies on photocatalytic conversion of nitrites and nitrates has been conceived for their full reduction to ammonia. The photo-assisted reduction of nitrite to

ammonia was first reported by Halmann and Zuckerman [18] in alkaline solutions by illumination with visible or UV light. The photocatalysts were $SrTiO_3$, TiO_2 and CdS, the latter used to improve visible light harvesting. The same reaction has been studied by Pandikumar et al. [19]. The authors proposed a TiO_2 photocatalyst added with Au nanoparticles. The advantage of Au addition resides in the modification of the electronic state of the semiconductor. The calculated band gap of the promoted materials effectively decreased from 3.35 to 2.86 eV improving light harvesting efficiency. The addition of Au allows the formation of donor states below the conduction band of TiO_2. Above a given concentration of Au, free electron properties are achieved and the bands are shifted to lower band gap. Very interestingly, the photocatalyst was immobilised in a polymeric matrix (Nafion), subsequently casted on a support. The composite device allowed even higher ammonia productivity, but the main novelty is the formation process, which allows the immobilisation of the catalyst with respect to conventional slurry configurations. This is one of the few papers on the topic dealing with this important practical issue.

The mechanism of nitrate photoreduction to ammonia, including the role of hole scavengers (HS), has been investigated in TiO_2 photocatalysts [20]. One of the major problems affecting quantum efficiency is the very fast recombination between electrons (e^-) and holes (h^+), generated upon light absorption, with respect to the rate of charge transfer and reaction. The use of an effective HS, such as oxalic acid, is reported as compulsory to improve the lifetime of electrons that are need for the target reactions. However, nitrate adsorption was found one order of magnitude lower with respect to the oxalate, which is therefore competitive for adsorption with the reactant over the catalyst surface. Hence, a compromise between effective hole scavenging and competition for adsorption has to be searched. The overall reduction of nitrate by oxalic acid is exoergonic, but characterised by a kinetic barrier due to the first reaction step:

$$NO_3^- + C_2O_4^{2-} \rightarrow NO_3^{2-} + C_2O_4^{\cdot-} \qquad\qquad 4)$$
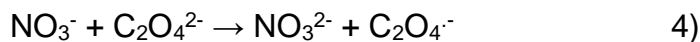
The oxalate radical can decompose to $CO_2^{\cdot-}$, which has suitable potential to reduce the nitrate itself. Furthermore, electrons in the conduction band can reduce H^+ to $H\cdot$, which is also a reducing agent for nitrates. Therefore, in acidic medium the nitrate can be primarily reduced by adsorbed hydrogen radicals, whereas in basic medium lower contribution of this route is expected and it can explain the lower ammonia yield. The reaction steps following the formation of the NO_3^{2-} intermediate are all exoergonic and predominantly lead to ammonia, that is the reason of the pressing selectivity problems of the process [20].

The photoreduction of nitrite to ammonia was also investigated in very diluted solutions (100 ppm) on CdS samples differently prepared and in case promoted with RuO_2 [21]. No activity was observed at very low or high pH (<2 or >10) and the addition of an inorganic hole scavenger such as sodium sulphite showed beneficial. The same authors proposed the photoreduction of nitrite and nitrate to ammonia over Ru/TiO_2 [21]. The co-catalyst was chosen among noble metals for electron affinity to act as electron trap. Some noble metals, *e.g.* Pt have very low overpotential for H_2, leading to rapid hydrogen evolution. Other metals, such as Ru have higher overpotential, leading to stabilized H_{ads} species to be used for reduction reactions. The investigation was later extended to other metals (Pt, Pd and Rh), deposed over TiO_2 by impregnation or photodeposition [22]. Ru confirmed the most selective to NH_3 when loaded by impregnation. This preparation procedure proved more effective than photodeposition and this fact was correlated to the higher average light absorbance shown by the samples. The authors proposed as first reaction step the reduction of water, with subsequent stabilisation or not of the H_{ads} species formed by the metal. The metal was considered an electron sink, forming an ohmic junction rather than a Schottky barrier with

the semiconductor. Mg, Fe, Cr and Co ions were also tested as dopants for TiO_2 by the same authors, but without a conclusive statement on the best catalyst formulation for the proposed reaction [23].

Nitrate are often removed by ion exchange, leaving a concentrated brine as byproduct. This has been treated to remove the concentrated nitrate over TiO_2 photocatalyst [24].

The photoreduction of nitrite and nitrate ions has been investigated over TiO_2 loaded with Pd and Ag [25].

$$5\ NO_2^- + 2\ H^+ \rightarrow N_2 + 3\ NO_3^- + H_2O \qquad\qquad 5)$$

$$2\ NO_2^- + 8\ H^+ + 6\ e^- \rightarrow N_2 + 4\ H_2O \qquad\qquad 6)$$

$$3\ NO_2^- + 3\ H_2O + 6\ h^+ \rightarrow 3\ NO_3^- + 6\ H^+ \qquad\qquad 7)$$
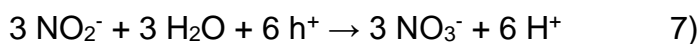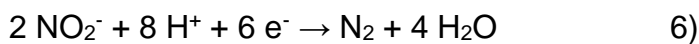
The disproportion of nitrite to nitrate and nitrogen was defined as the main pathway over bare TiO_2 and it was characterised by low turnover frequency [26]. Pd addition to TiO_2 significantly improved the rate of disproportion, but the formation of nitrate as byproduct is undesirable. Holes formed after photopromotion of an electron from the valence to the conduction band of the photocatalyst act as electron acceptor and are responsible for the oxidation semireaction. They have to be rapidly filled during the reaction in order to limit the very fast electron-hole recombination and to inhibit the oxidation semireaction. Therefore, the authors suggested the use of a HS, such as sodium oxalate, in order to limit nitrate formation [25].

$$e^- \text{-} h^+ + HS \rightarrow e^- + HS_{OX}^+ \qquad\qquad 8)$$

$$NO_3^- + 2\,e^- + 2\,H^+ \rightarrow NO_2^- + H_2O \qquad\qquad 9)$$
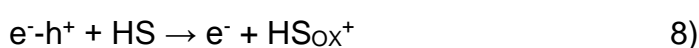
However, the proposed solution was not sufficient to limit the undesired selectivity to nitrate. Alternatively, the coupling with a second catalyst active for nitrate photoreduction was proposed, in order to achieve significant nitrite and then nitrate conversion to N_2 [25]. Ag/TiO_2 and Cu/TiO_2 photocatalysts were compared for nitrate photoreduction. Both were active, but Cu led to the formation of undesired ammonium ions depending on pH. Au was also tested, but it was ineffective for the proposed reaction, acting mainly as an electron-hole recombination centre than as a co-catalyst. A reaction scheme in which Pd/TiO_2 accomplished nitrite disproportion and Ag/TiO_2 photoreduced the formed nitrate back to nitrite was proposed, yielding 70% N_2 by nitrite photoreduction [25].

The simultaneous photoreduction of nitrites and oxidation of ammonia to N_2 was investigated by using a Ag-Ce modified TiO_2 catalyst. The best material formulation was constituted by 0.1 wt% of both dopants, which were involved in the electron transfer chain. A one-electron process accompanies the reduction of Ce^{4+}, formed by photogenerated holes, to Ce^{3+}, therefore, the redox cycle of Ce ions was useful to enhance charge separation and transport. Furthermore, Ce ions size did not allow their incorporation into the lattice. Their clustering on titania surface was also responsible of a red-shift of the semiconductor absorption edge. Interestingly, the authors also compared catalyst performance by irradiation under solar light with respect to UV, achieving *ca.* 45% and 60% removal of total nitrogen (TN), respectively [27].

Ag/TiO_2 showed very active for nitrite reduction and most of all selective towards N_2, without significant over-reduction to ammonia [28]. The optimum metal amount was 1 wt% and photodeposition over the semiconductor led to better activity with respect to chemical reduction with KBH_4. The reason was searched in the higher dispersion of the metal. The

Ag Fermi level is lower than that of TiO_2, so that the photogenerated electrons may transfer to the Ag particles with formation of a Schottky barrier for the efficient separation of the photogenerated charges. Excessive metal loading may either induce a shielding effect inhibiting light absorption by the semiconductor, or bigger metal particles act as recombination centres. Relatively high nitrite removal rate was achieved (19 mmol/min g_{Ag}). The presence of competitive anions commonly found in water did not influence activity appreciably, indicating that competition for adsorption was not critical. By contrast, pH played a major role. Indeed, the isoelectric point of TiO_2 is *ca.* 6.25. At pH < 6.25 the surface of the catalyst is positively charged, favouring nitrite adsorption. By contrast, at higher pH the negatively charged surface inhibits the adsorption of the reactant. On the same basis the authors interpreted the significantly different effect of the added hole scavengers. Oxalic acid was the most effective, inducing acidification of the medium, at difference with the corresponding salts. A mechanism for the role of the HS was also proposed. During oxidation of the HS to CO_2, intermediate radical $CO_2 \cdot^-$ surface species form, which are much stronger reductants than the electron itself.

$$2\ NO_2^- + 8\ H^+ + 6\ e^- \rightarrow N_2 + 4\ H_2O \qquad\qquad 10)$$

$$C_2O_4^{2-} + h^+ \rightarrow CO_2 + CO_2^{\bullet-} \qquad\qquad 11)$$

$$2\ NO_2^- + 8\ H^+ + 6\ CO_2^{\bullet-} \rightarrow N_2 + 4\ H_2O + 6\ CO_2 \qquad 12)$$

$$2\ NO_2^- + 3\ C_2O_4^{2-} + 8\ H^+ \rightarrow N_2 + 6\ CO_2 + 4\ H_2O \qquad 13)$$
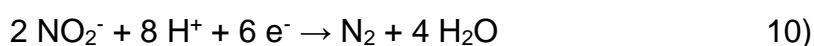
A bit higher attention was focused on nitrate photoreduction, even if the tolerable limit of this pollutant is one order of magnitude higher than that of nitrite.

Also in this case the first attempts were focused on the photoreduction of nitrates to ammonia on Ag/TiO_2 in the presence on 2-propanol [29] or formic acid [30] as HS. Nitrate reduction was observed after Ag^+ reduction and deposition on TiO_2 from the $AgNO_3$ precursor [29]. Nitrate conversion started after completion of silver reduction, with the need of a HS, since nitrate cannot exploit directly photogenerated electrons at difference from Ag^+.

Ag/TiO_2 catalysts were investigated for nitrates photoreduction [31, 32]. Formate was used as hole scavenger. Ag addition led to a localised surface plasmon resonance, leading to absorption bands in the visible region of the spectrum [31]. The apparent reaction order was one for both formate and nitrate removal reactions. The optimal photocatalyst amount was 1 g/L, offering sufficient photocatalyst area and limiting the shielding effect occurring at higher particle density in the solution. Also in this case, the effect of pH was major. Both formate and nitrate should be adsorbed on the surface, so at pH>10 the negatively charged surface was unsuitable for nitrate removal. It should be noticed that Ag addition modified the isoelectric point of the material. The formation of the $CO_2 \cdot^-$ radical through oxidation of the HS was confirmed by electron paramagnetic resonance. This radical was rapidly quenched by either oxygen or nitrate.

It was demonstrated that hole trapping centres are more abundant on {0 0 1} facets of anatase TiO_2, while more electron trapping sites are present on {1 0 1} facets [33–35]. This concept has been applied by Sun et al. [36] to enhance charge separation through materials engineering, by selectively depositing Ag nanoparticles onto {1 0 1} facets of anatase nanocrystals. The activity of the prepared samples was compared to Ag/TiO_2 P25 under simulated solar light. The first order kinetic constant was effectively increased. The samples were tested in presence of various HS such as HCOOH and organic compounds simulating possible pollutants for water, such as humic acid, dyes and benzene.

Almost quantitative photoreduction of nitrates to N_2 has been reported with Ag/TiO_2 catalysts in acid medium and in the presence of formic acid [37]. Also in this case, $CO_2\cdot^-$ was addressed as the reducing species. Indeed, the redox potential of the couple $CO_2/ CO_2\cdot^-$ is calculated as -1.8V, to be compared with $E°_{CO2/HCOO-}$ = -0.2V and with the potential of photogenerated electrons which is -0.29V [38, 39]. Therefore, $CO_2\cdot^-$ is suitable to reduce both nitrate and nitrite to molecular nitrogen, being $E°_{NO3-/N2}$ = 1.25V and $E°_{NO2-/N2}$ = 1.45V.

Ag can thus be considered as a very effective co-catalyst for the photoreduction of nitrates, promoting high selectivity to N_2. However, repeated reaction cycles demonstrated poor recyclability [40], which is a must for practical application. Ag_2O was then tested, showing promising stability after 8 reaction cycles. Very high metal oxide loading was proposed by Ren et al. [40], up to 12.5 wt%, after which the shielding effect was unacceptably high. Different conceptual schemes have been proposed for the two catalytic systems (Fig. 1).
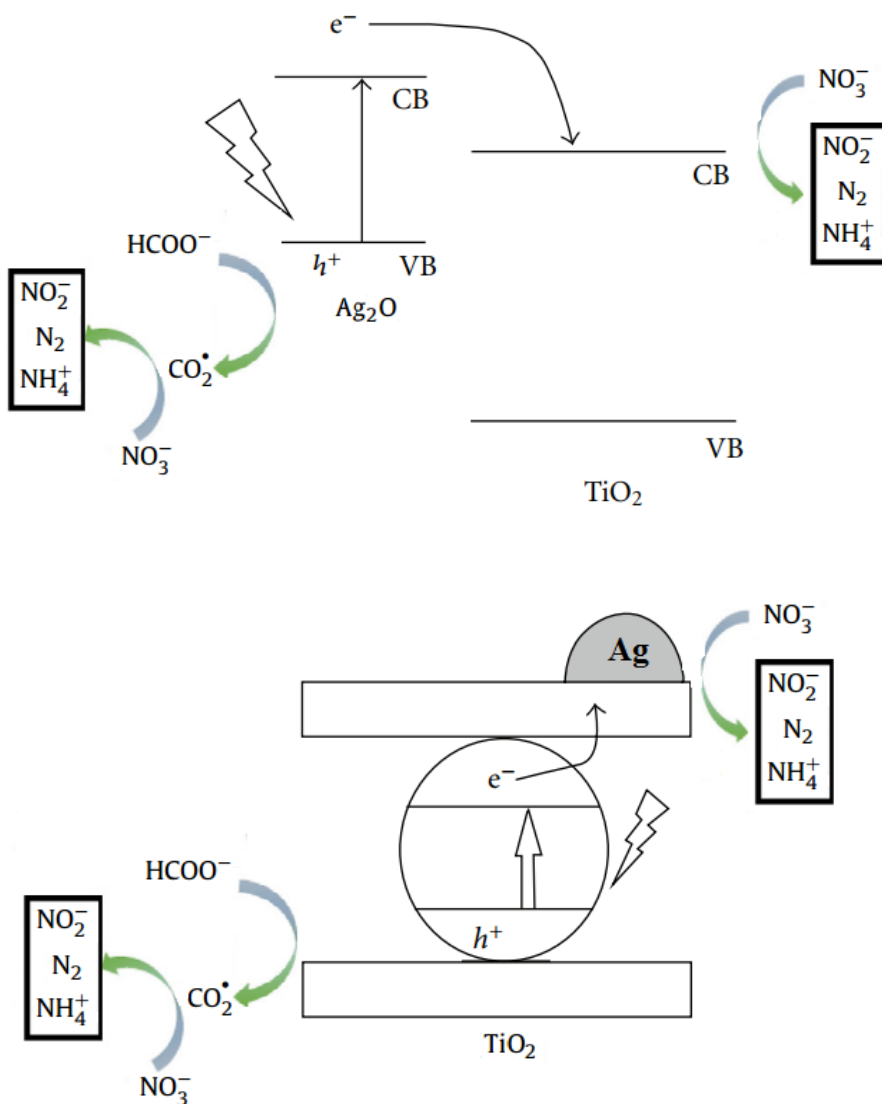
Fig. 1. Schematic representation of reaction mechanisms for Ag_2O/TiO_2 and Ag/TiO_2 during the photoreduction of nitrates. Readapted from [40].

Ag-doped TiO_2 samples prepared on both P25 and Hombikat materials proved more active and selective to N_2 with respect to undoped photocatalysts for the reduction of nitrates [41]. Fe- and Cu-doped catalysts were also compared, but showed less promising. Fe^{3+} in particular was interesting as possible trap for both electrons and holes, possibly leading to Fe^{2+} and Fe^{4+} species. However, the conversion plot was characterised by an induction

period after which the same behavior of the bare support was observed. This was attributed to leaching of Fe, as proven by chemical analysis of the spent samples. The role of the HS was also considered, obtaining the highest activity for formic acid, with lower selectivity to N_2 than acetic acid or sodium formate and acetate. The lower selectivity was in line with the much higher conversion achieved (100%) with respect to 10-20% of the rival compounds. Activity increased with temperature, but with decreasing selectivity to N_2 (nitrite formed in negligible amount, while the main byproduct was ammonium). The apparent activation energy was 32 kJ/mol, suggesting that a physical or chemical step was rate-limiting, rather than a photochemical step which would be temperature independent. Furthermore, decreasing particle size of the semiconductor showed beneficial to increase surface area and to improve charge transport towards the surface.

Anderson [42] reported a kinetic investigation on 1 wt% Au/TiO_2 for the photoreduction of nitrate solutions in the presence of oxalic acid as hole scavenger. An induction time for nitrate conversion was observed if the solution was not flushed with inert gas, indicating competition between nitrate and oxygen reduction by photogenerated electrons, although this is a controversial point. By contrast, the consumption of the HS was the same. From the kinetic point of view, nitrate conversion rate was almost independent from the concentration of the HS and of the nitrate solution. The reaction rate may be expressed as power law or, better, through a Langmuir Hinshelwood model. An apparent activation energy was found *ca.* 20 kJ/mol, which is mainly ascribed to the reactant adsorption term. Nitrite was formed as intermediate in relatively low concentration (5 ppm), which remained stable, thus with equal formation and removal rates, until nitrate was completely converted. After full nitrate conversion nitrite reduction also started, revealing that there is poor competition for surface adsorption between these two compounds. H_2 formation was a competitive reaction, occurring through this simplified scheme (Fig. 2) and favoured by the presence of organic HS, as well detailed elsewhere [43–45].
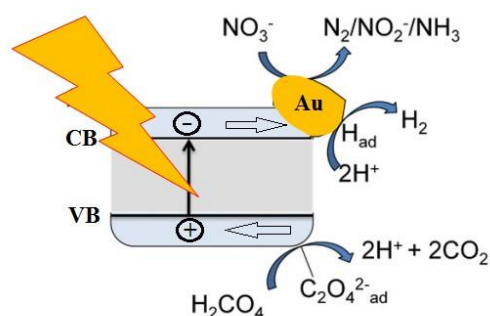
Fig. 2: Simplified reaction scheme for the oxidation of the hole scavenger and the competitive reduction of nitrate and of protons. Readapted from [42].

Gao et al. [46] proposed bimetallic TiO_2 catalysts for the photoreduction of nitrates. Pt, Pd, Ni and Cu were used singly or coupled as co-catalysts. The authors concluded that Ni-Cu formulations were more effective, with specified metal ratio and total content. However, when comparing the results obtained with various formulations one may notice that the major role of bimetallic systems was to enhance the rate of nitrate photoreduction, but unfortunately depressing the selectivity to N_2.

A double catalytic system was also proposed for the photoreduction of nitrate through a mixed catalytic-photocatalytic system [47]. Pt/TiO_2 was found ineffective for the reaction. After the addition of $Sn-Pd/Al_2O_3$ as a second catalytic system and with the use of ethanol as hole scavenger, significant nitrate conversion was observed, without nitrite formation and with limited selectivity to ammonia. Based on cross blank testing, it was found that the bimetallic catalyst was active for the catalytic reduction of nitrate under very mild conditions.

Pt/TiO$_2$, though not directly active for the photocatalytic reduction of nitrates, was very active for the reduction of water to H$_2$, mediated effectively by ethanol as HS. Through the coupling of the two systems H$_2$ was produced photocatalytically and catalytically used as reactant for the reduction of nitrate. The separate H$_2$ photocatalytic formation and use for nitrate reduction was also accomplished with Pt/TiO$_2$ + Sn-Pd/Al$_2$O$_3$ using real ground water as substrate [48].

$$2\ H^+ + 2\ e^- \rightarrow H_2 \qquad\qquad 14)$$

$$NO_3^- + 5/2\ H_2 \rightarrow 1/2\ N_2 + 2\ H_2O + OH^- \qquad 15)$$
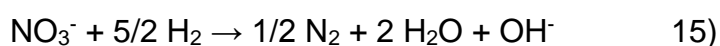
The authors observed worse performance in the case of a real substrate with respect to pure nitrate solutions. The negative effect of cations was excluded, whereas the main competition was found with anions. In particular, the activity of the Pt/TiO$_2$ photocatalyst was significantly decreased in the presence of organic compounds other than glucose, added as HS, and with SO$_4^{2-}$ and SiO$_3^{2-}$. A combination of Cl$^-$ + SO$_4^{2-}$ + SiO$_3^{2-}$ was detrimental for the Sn-Pd/Al$_2$O$_3$ catalyst. The latter ion is thought to form oligomers adsorbed over the catalyst surface.

The same researchers later developed a similar solution able to extend light harvesting to the visible part of the spectrum [49]. Indeed, they used Pt/SrTiO$_3$:Rh with different hole scavengers for H$_2$ production and the same Sn-Pd/Al$_2$O$_3$ catalyst for the catalytic reduction of nitrates. A more reasonable increase of selectivity to ammonium with increasing nitrate conversion was reported. However, increasing ammonium production was evident after repeated reaction cycles. The proposed reaction mechanism is reported in Fig. 3. Among the HS, formic acid was the most effective.
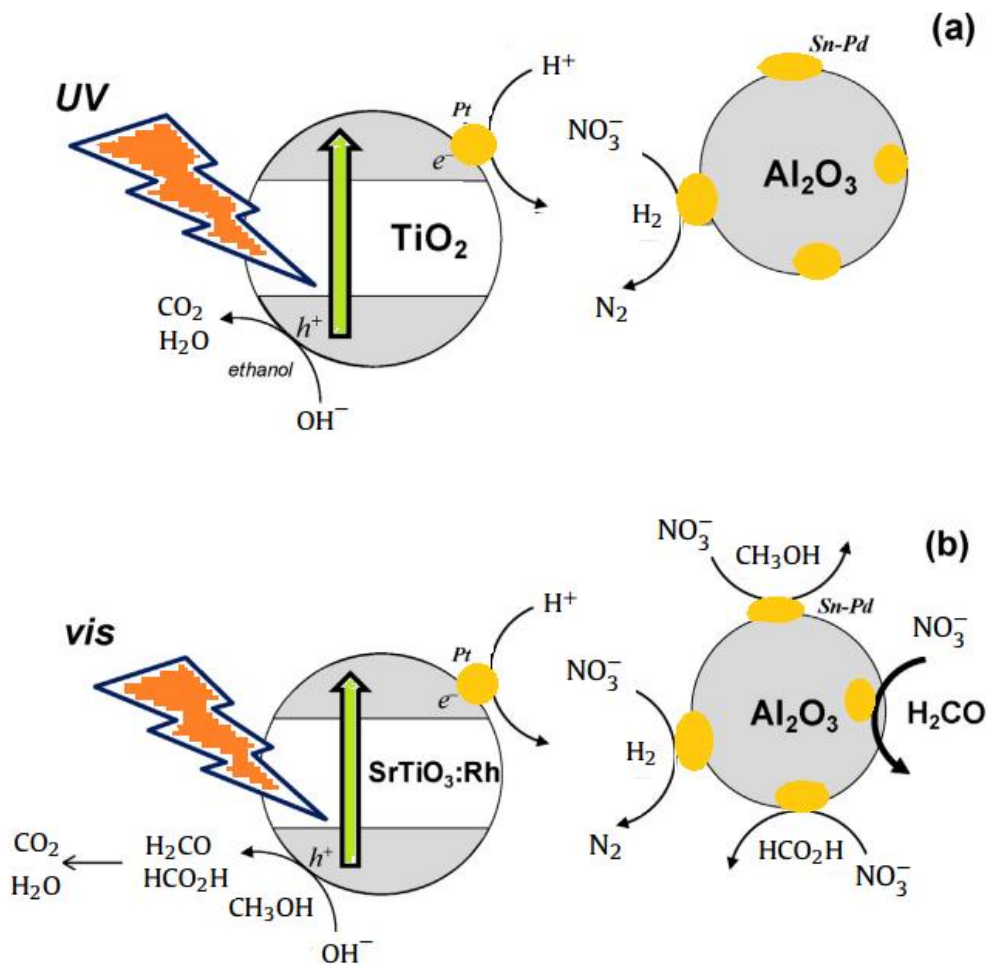
Fig. 3: Simplified reaction scheme for coupled catalytic and photocatalytic nitrate reduction. Readapted from [49].

The photoreduction of nitrate to ammonia was formerly investigated over various metal loaded TiO_2 photocatalysts [50]. The same authors later focused on the selective reduction of nitrate to N_2, which represents a much more appealing process for environmental remediation [51]. Various metals were added to TiO_2 and the reaction was performed with oxalic acid as HS. The best results were reported for a bimetallic Pd-Cu formulation, operated at pH=11. However, the modification of pH during the reaction due to CO_2 formation by oxidation of the oxalate scavenger limited the reaction rate. A procedure called

pH swing was adopted, opening the batch reactor tubes to outgas CO_2 and adding again NaOH, to recover the original activity. This paper represents an exception for operation under basic conditions, most reports privileging acidic pH to favour the photoreduction reaction with low ammonia selectivity.

The catalytic and photocatalytic reduction of nitrate were compared over $Pd-Cu/TiO_2$ samples, with formic acid as hole scavenger [52]. NO_2^- was obtained by using H_2 as reducing agent for the catalytic reaction carried out at room temperature. An induction time was observed for the catalytic process in the presence of H_2. The simultaneous presence of $H_2+HCOOH$ was beneficial for nitrate removal rate. $4.2\%Pd-1.2\%Cu/TiO_2$ was the best performing material under H_2 in dark conditions. The reaction seems structure sensitive, with optimal required Pd crystal size. In dark conditions formic acid was ineffective for nitrate reduction. The catalytic process formed ammonium in different amount depending on pH and it was higher than allowed by regulations. Activity was higher under irradiation and a mechanism based on H-based reducing species formed in situ was proposed [52]. The selectivity for ammonia production over bimetallic Pd-Cu catalysts was also investigated [53].

The selective photocatalytic reduction of nitrate to nitrogen was studied by Li et al. over bimetallic $Pt-Cu/TiO_2$ samples in the presence of benzene as HS [54]. The choice of benzene was made on the basis of its harmfulness as pollutant and on its recalcitrant behavior towards biotic degradation routes. Its photocatalytic oxidation goes through intermediates such as phenol and quinone, short chain acids and finally the complete mineralisation. No nitrate conversion was observed in the absence of HS and, possibly, oxidized radicals were directly involved in nitrate reduction as previously reported. The authors attributed a direct redox action to metallic Cu, which can reduce the nitrate ion to nitrite, being oxidized to $Cu^{\delta+}$. The latter ion is photocatalytically reduced by photoproduced

electrons in the presence of the HS. Indeed, after benzene consumption nitrites are oxidized back to nitrates over the semiconductor surface. Selectivity to N_2 was observed in the case of bimetallic formulations, only [54]. The role of Pt seemed double. On one hand it could contribute to the reduction of the oxidized $Cu^{\delta+}$ ions. Furthermore, it is believed the main responsible of the reduction of the nitrite ion, which preferentially adsorbs over this metal, to the desired N_2 product or to the undesired NH_3. Therefore, the Cu/Pt ratio should be carefully optimised, since higher Cu content improved the nitrate reduction rate, but unfavoured the subsequent nitrite photoreduction.

A similar system based on Pd-Cu/TiO_2 catalysts was proposed and operated in the presence of H_2 and H_2+CO_2 [55], as described in Fig. 4. The effect of H_2 on activity and selectivity to ammonium byproduct was discussed, and in general it was found to improve the reduction of the nitrite intermediate. The pH was very important to ensure proper adsorption of both the reactant and the intermediate for further conversion. The pH was fixed around 5 by using CO_2 as sustainable buffer, perfectly tolerable in drinking water. The use of different HS was also discussed, the most effective one confirming formic acid. It should be also noticed that the different HS may induce modification to the pH, and hence determine different adsorption of reactants and intermediates. This is particularly relevant due to possible pH modification during reaction. The buffering effect of CO_2 was beneficial also from this point of view. Unfortunately, humic acid showed the less effective HS, although in principle very promising because it naturally occurs in groundwater [41].
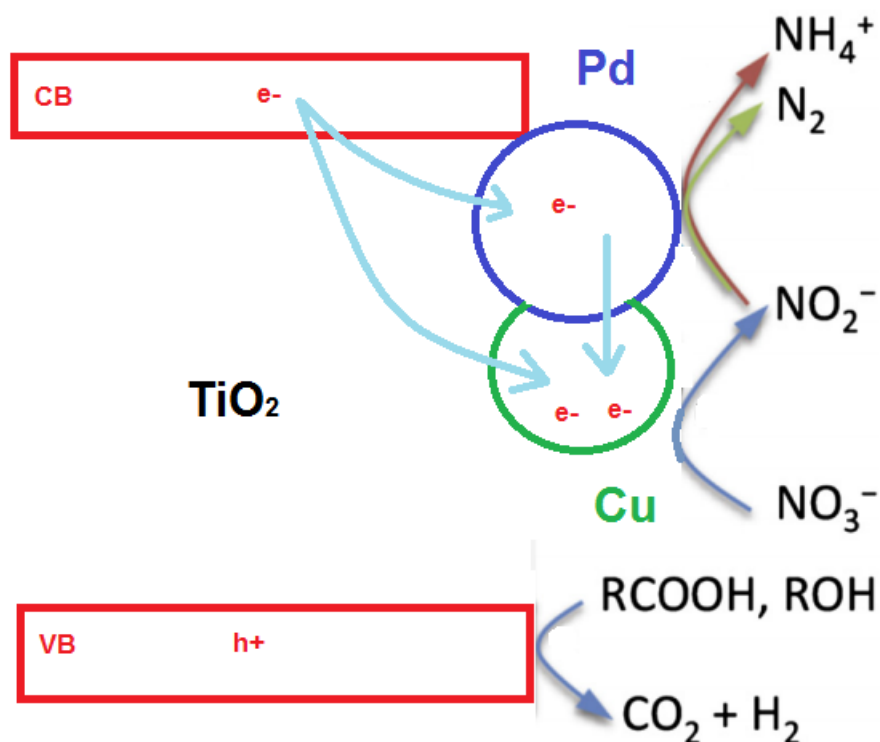
Fig. 4: Schematic representation of Pd-Cu/TiO₂ used for nitrate photoreduction. Readapted from [55].

Noble metals are usually reported as electron sinks for this application. An exception was constituted by a Fe/TiO$_2$ photocatalyst, which was reported as effective for the selective photoreduction of nitrates with significant selectivity to N$_2$ [56]. *Ca.* 70% selectivity to N$_2$ was achieved at 52% nitrate conversion using chemically reduced 0.5 wt% Fe in the presence of formic acid as HS.

Different co-catalysts or doping ions were tested for TiO$_2$ [57], *i.e.* Zn^{2+}, Cr^{3+} and Cu^{2+}. At difference with Cr^{3+}, which was able to intercept only one type of charge carrier, Cu^{n+} may be able to drain both photoproduced electrons and holes. A variation of its oxidation state upon irradiation was visually observed, the catalyst colour changing from blue to pink upon irradiation and back to blue in dark conditions. On this basis the authors explained the higher activity of Cu^{n+} with respect to Cr^{3+}, however accompanied by unacceptably high selectivity

to ammonia. The best results were achieved with Zn^{2+}, especially in terms of selectivity. This ion, with very similar ionic radius with respect to Ti^{4+} can enter in the anatase lattice as substituent, on one hand allowing promotion with higher dopant amount, and further inducing a permanent electric field in the sample. A Schottky barrier can then form between ZnO and TiO_2 improving the lifetime of the photogenerated charges. The effect of dissolved oxygen was also investigated, O_2 being a possible electron acceptor and thus competing with nitrates for reduction. The reaction can be performed in the presence of oxygen, but the overall process efficiency is improved at decreasing oxygen concentration in the reaction medium [57].

Bi^{3+} was also proposed as dopant for TiO_2 [58]. When added using mild preparation methods separate oxide phases form, without isomorphic substitution. Based on photoluminescence experiments the role of Bi ions was essentially of charge trapping, with optimal loading 1.5 wt%. As well, formic acid was used as electron scavenger confirming the role of $CO_2 \cdot^-$ as reducing agent for the nitrate. Also, under acidic conditions adsorbed hydrogen radicals may form, which proved able to reduce nitrates.

Additionally, unconventional TiO_2 phases, such as Brookite and a mixed Anatase-Brookite mesoporous samples were tested for this application, with and without formic acid as HS [59]. The results seem interesting and deserve deepening, but the authors claim an absorption band in the visible region, which is consistent with the presence of undecomposed organic precursors, documented by IR bands of the calcined samples. These organic species can act as HS during the nitrate photoreduction tests in absence of formic acid, explaining the much higher activity observed with respect to TiO_2 P25.

A composite photocatalyst, $Cu\text{-}MgTiO_3\text{-}TiO_2$ was proposed for nitrate photoreduction in the presence of oxalate, oxalic acid and ethanol as HS. The authors evidenced negligible activity in the absence of the metal, considered an electron sink, and the organic compound,

removing holes. Among the scavengers, the oxalate ion proved better in appropriate concentration. Too concentrated solutions instead prevented the effective nitrate adsorption over the surface [60].

A completely different catalytic system was proposed by Kato and Kudo [61]. They proposed various tantalates, given their superior photocatalytic activity with respect to TiO_2. They showed that $KTaO_3$ was the most active catalyst, with or without the addition of NiO as co-catalyst in various amounts. These catalytic systems were effective for the photoreduction of nitrates without the addition of any hole scavenger, directly from water. Non negligible nitrite and ammonia (minor) formation was also observed and ammonia oxidation to N_2 can be also possible by means of oxidising holes.

$NaTaO_3$ was also used after addition of various Pd amounts [62]. The addition of Pd induced a decrease of the calculated band gap, claiming operation under visible light irradiation. Apparently, nitrate conversion was almost complete after *ca*. 2 h irradiation, but no specifications about selectivity are given.

Attempts to improve visible light harvesting were described also by Mishra et al. [39]. In general, the reduction of the band gap of titania is desirable to increase the utilisation of solar light. Different strategies were adopted in other applicative fields, such as doping with non-metals (mainly N-doping) or proposing double oxides. TiO_2 was doped simultaneously with WO_3 and N, by simultaneous controlled hydrolysis of the Ti and W precursors in the presence of NH_3. 2 wt% WO_3 showed the optimal amount of dopant, which however did not modify light absorption properties to a much greater extent than pure N-doping. On the contrary WO_3 deeply affected the surface acidity and surface OH concentration of the sample. The effect of Cl^- presence was also investigated and it seemed to enhance the photocatalytic reduction efficiency of the system. Completely different $CuInS_2$ materials were

reported with low band gap and significant activity for nitrate conversion, although poor details on the mechanism and on selectivity were provided [63].

Different sulphides were also used for nitrate reduction under visible light, such as $CuFe_{0.7}Cr_{0.3}S_2$ [64]. Different single co-catalysts were added, among which Au and Ru decreased conversion, whereas Ag, Pt and Pd increased NO_3^- removal rate. Bimetallic formulations were also proposed and the best compromise between nitrate conversion and N_2 selectivity was 0.75%Pd-3.0%Au. Hypotheses on the reason why Au addition was detrimental alone and favourable in bimetallic catalysts have not been convincingly provided.

Hollandites have been also tested [65]. These structures are characterised by a one dimensional channel of $M^{IV}O_2$ with rutile-type MO_6 octahedra. The channels are occupied by alkaline or alkaline earth cations and the M^{IV} ion is partially substituted with di- or trivalent cations. A $K_{1.8}Ga_{1.8}Sn_{6.2}O_{16}$ formulation has been specifically proposed as active for the photocatalytic reduction of nitrates in presence of methanol. The selectivity to N_2 has been detailed by using isotopically labelled $H^{15}NO_3$ as substrate for reduction and analysing $^{15}N_2$ as products by mass spectrometry. The pivotal effect of pH was confirmed, mainly affecting selectivity. NO_2^- was the main product at pH=7, but its selectivity decreased to negligible values at pH=3. Apparently, the HS was selectively oxidised to HCOOH, without CO_2 detection.

More recently, a layered perovskite structure $BaLa_4Ti_4O_{15}$ with Ni co-catalyst was investigated [66]. The direct photolysis of nitrate to nitrite and oxygen occurred in the absence of Ni and for $\lambda < 300$ nm. Yield of N_2 was effectively improved, up to 80% after 4 h irradiation, by addition of Ni or Cu, the latter showing higher selectivity to nitrite. However, the reported effect of Cu seems contrasting with results reported for Cu/TiO_2, which mainly promoted the formation of NH_4^+. The reason for this discrepancy, besides the different

semiconductor, may be searched in the different pH conditions reported by the authors (pH=7-12) [66]. The effect of increasing pH was limited by addition of H_3BO_3 as buffer.

Different materials were reported for the photoreduction of nitrates, such as $H_2Ti_4O_9$, in case added with Pt and CdS to improve visible light absorption. More appropriately, CdS acted as hole scavenger rather than a co-catalyst, because significant amounts of Cd^{2+} and SO_4^{2-} were found in the solution [67]. Pillared materials such as $H_2Ti_4O_9$ and $H_4Nb_6O_{17}$ incorporating Pt or CdS were also tested under UV and visible light [68, 69].

From the above reported records it appears that some candidates are available for the photoreduction of nitrite and nitrate ions with suitable selectivity to N_2. However, only few papers deal with strictly practical issues, needed for scale up of the technology. For instance, the application to real waste water was investigated by de Bem Luiz et al. [70], together with the proposal of a kinetic model which is a preliminary entry information for the design of a water treatment reactor on the real scale. Kinetic modelling was carried out with a simplified Langmuir Hinshelwood approach, solved by linearisation. It was applied to data collected on a ZnO-TiO_2 photocatalyst in the presence of formic acid as HS, without adjusting pH during reaction. The pH varied from 2.5 to ca. 3.5 in *ca.* 2 h, due to H^+ depletion according to the stoichiometry of the reaction. The model was later applied to a real substrate, constituted by a Brazilian poultry slaughterhouse wastewater obtained after preliminary coagulation + flocculation and aerobic biological treatment. At that stage only nitrate, colour, turbidity and coliform species were above the limits. The substrate was filtered before photoreaction over commercial cartridges. The photocatalytic activity for waste water treatment was lower than that predicted by the model, likely due to competitive adsorption over catalyst surface and competition for electrons and holes [70].

Finally, for the practical application in the treatment of drinking and waste water, slurry is not the best choice due to separation problems. Forming is a major issue, only rarely addressed

in the literature. An example of film formation and the relative photoreactor design has been reported recently [71]. TiO_2 and Ag-TiO_2 films were compared, the former achieving *ca*. 45%, the latter *ca*. 75% nitrate removal using formate as HS, with almost quantitative selectivity to N_2.

Summarising, the catalytic systems discussed for the photoreduction of NO_x^- are collected in Table 2.

Table 2: Examples of catalytic systems reported for the photoreduction of NO_x^-.

Catalyst	Co-catalyst	Conversion NO_3^-, NO_2^- (%)	Selectivity N_2 (%)	Reference
TiO_2	Au	-	-	19
TiO_2	-	50	NH_3	20
CdS	Ru, Pd, Ir	-	NH_3	21
TiO_2	Ru	-	NH_3	22
TiO_2	Fe, Cr, Co, Mg ions	-	NH_3	23
TiO_2	-	80	-	24
TiO_2	Au, Ag, Pd, Cu, Pt	Ca. 90	70	25
TiO_2	Pd, Cu, Ru, Ag, Au	100	35	26
TiO_2	Ce, Ag	50	-	27
TiO_2	Ag	100	99	28,30
TiO_2	Ag	100	variable	31
TiO_2	Ag	90	-	32
TiO_2	Ag	96	100 (absence of nitrite and ammonia)	37
TiO_2 (mesoporous)	W,N	100	> 95	39
TiO_2	Ag_2O	99.6	88.4	40
TiO_2	Cu, Fe, Ag	100	96	41
TiO_2	Au	< 50	-	42

TiO$_2$	Ni, Cu	17	100	46
TiO$_2$	Pt, Sn, Sn-Pd (photocatalyst) + Rh (catalyst)	39	90	47-49 (photocat + cat. process)
TiO$_2$	Pt, Pd, CuO, Ni, Au, Ag, Cu	90	NH$_3$	50
TiO$_2$	Cu, Pt, Pd, au	56	98	51
TiO$_2$	Pd, Cu	98	90	52
TiO$_2$	Cu, Pd	95	NH$_3$	53
TiO$_2$	Pt, Cu	-	80	54
TiO$_2$	Pd, Cu	95	50	55
TiO$_2$	Fe	52	72	56
TiO$_2$	Bi	80	NH$_3$	58
TiO$_2$ (mesoporous)	-	60	5% NH$_3$, 20% NO$_2^-$	59
MgTiO$_3$ - TiO$_2$	Cu	39	-	60
KTaO$_3$	Ni	-	-	61
NaTaO$_3$	Pd	100	-	62
CuInS$_2$	-	75	-	63
CuFe$_{0.7}$Cr$_{0.3}$S$_2$	Rh, Au, Cu, Ag, Pt, Pd	100	65	64
K$_x$Ga$_x$Sn$_{8-x}$O$_{16}$	-	30	100	65
BaLa$_4$Ti$_4$O$_{15}$	Ni, Ag, Cu	-	80 (yield)	66
H$_2$Ti$_4$O$_9$/CdS	-	100	NO$_2^-$, NH$_3$	67
TiO, H$_x$Nb$_y$O$_z$	Pt	100	20	68
H$_x$Nb$_y$O$_z$	CdS	60	Ca. 60	69
TiO$_2$	Zn	92	95	70
TiO$_2$	Ag	70	99	71

3 – Photodecomposition and photo-oxidation of ammonia/ammonium

Aqueous ammonia is a major aquatic pollutant present in livestock waste and significantly present also in heat power plants, chemical facilities and sewage farms. Both ammonium, NH_4^+, and its conjugate base, NH_3, are present in water according to the equilibrium

$$NH_3 + H_2O = NH_4^+ + OH^- \qquad\qquad 16)$$

In the case of aqueous ammonia solution (15 M) the molecular NH_3 predominantly exists (15 M) while ammonium ion, NH_4^+, hardly exists (1.6×10^{-2} M) according to the equilibrium constant ($K_b = 1.8 \times 10^{-5}$) at 298 K.

The amount of nitrogen contained in livestock manure, together with chemical fertilisers, strongly increases with the rapid development of modern agriculture and industry productivity, and generates a dangerous accumulation of nitrogen-containing nutrients in soil and groundwater. Moreover, it is well known that ammonia is toxic to fish, even at low concentrations [72].

The presence of NH_3/NH_4^+ in natural water may cause eutrophication and enhance algal growth. High concentrations of ammonia in potable water may lead to the reduction in the efficiency of chlorine disinfection, producing bacteria growth and corrosion of copper pipes. Due to the acute toxicity, disagreeable taste and smell at trace levels the maximum concentration of NH_3/NH_4^+ in potable water as set by World Health Organization at 1.24 ppm.

The current methods for removal of NH_3/NH_4^+ include breakpoint chlorination, ion exchange, membrane separation, air stripping, chemical oxidation and biological nitrification to NO_2^- and NO_3^- and subsequent denitrification to N_2. Often ammonia is not removed completely and one or more nitrogen-containing compounds persist within the waste stream after the treatment. Although breakpoint chlorination can convert aqueous ammonia to nitrogen, the

formation of harmful by-products, such as trihalomethanes and haloacetic acids, must be suppressed and treatment of residual chlorine is required. Membrane separation technology and ion exchange method are separation enrichment technologies, which could produce high concentration wastewater that is even more difficult to treat. Catalytic wet oxidation of ammonia has been reported, in which the treatment is conducted under relatively high pressure and temperature, e.g. 2.0 MPa and 500 K. As a result, industries are seeking robust methods with better efficiency, lower costs and lower time for disinfection and decontamination of water.

Compared with nitrobacterial process, photocatalytic nitrification process is notably advantageous due to its character of keeping high oxidation ability in high saline wastewater. The photocatalytic reaction seems to be the right way for decreasing ammonia concentration in waste water [73]. Most studies focused on ammonia photocatalytic oxidation to possible products such as N_2, N_2O, NO_2^-, NO_3^- [73–82]. However, as seen in the previous paragraphs, the amount of nitrate and nitrite in water must be kept below a definite value, so selective oxidation to N_2 is highly recommended [26, 83]. Currently, only a few studies focused on the photocatalytic ammonia decomposition to nitrogen and hydrogen. They were predominantly intended as a way to produce hydrogen, but, of course, they may be interesting also as a way to eliminate such pollutant from gas or liquid streams. Indeed, ammonia attracted great attention as a possible energy source due to production of hydrogen from its decomposition. The photocatalytic decomposition of ammonia was presented as a very promising way to produce hydrogen at low cost, using solar energy, which is essentially free, and because ammonia can be transported and stored in liquid phase, as severe conditions are not necessary for its liquefaction. Moreover, hydrogen content percentage in one molecule (NH_3: 17.6%) is high in comparison with other possible hydrogen storage carriers, such as liquefied petroleum gas (LPG).

Finally, from a thermodynamic point of view, the decomposition of ammonia is better than direct water splitting ($\Delta G° = +237$ kJ mol^{-1}) showing a significantly lower value of Gibbs free energy:

$$2/3\ NH_{3(g)} \rightarrow H_{2(g)} + 1/3N_{2(g)} \qquad \Delta G° = +11\ \text{kJ mol}^{-1}; \qquad\qquad 17)$$

$$2/3\ NH_{3(aq)}\ (1\ \text{mol dm}^{-3}) \rightarrow H_{2(g)} + 1/3N_{2(g)} \qquad \Delta G° = +18\ \text{kJ mol}^{-1}. \qquad\qquad 18)$$
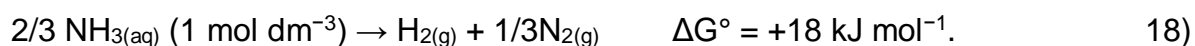
Moreover, the alternative hydrogen production by photocatalytic water splitting using solar energy cannot proceed without sacrificial carbon-containing materials such as methanol or ethanol.

The photocatalytic ammonia decomposition proceeds at room temperature and atmospheric pressure by using only clean and inexhaustible light energy. Titania is, definitely, the main photocatalyst studied in the last twenty years.

The generally accepted benchmark for solar-to-hydrogen efficiency under solar irradiation is 10% for practical implementation. Therefore, shifting the absorption edge of TiO_2 to include more of the visible light, which composes a greater portion (45%) of the solar spectrum, is one of the prerequisites to enhance the solar energy conversion efficiency. The surface plasmon resonance (SPR) effect is defined as the collective coherent oscillation of the free electrons on noble metal nanostructures induced by visible light irradiation. It can enhance the localised electric field in the proximity of the metal particles, whereas the interaction of localised electric fields with a neighbouring semiconductor allows for the facile formation of electron–hole (e^-–h^+) pairs in the near-surface region of the semiconductor. This is one of the most popular ways in which solar light harvesting can be improved.

Finally, although the photocatalytic removal of ammonia from water shows attractive prospects, using TiO_2 as a photocatalyst, meeting the practical application requirement is still a challenge because of the difficulty of separating suspended TiO_2 particles from

aqueous solution. For easier handling, recycling and safety, it is advisable to immobilise the photocatalysts on a solid carrier. Some practical examples of application of NH_3 (photo)decomposition and (photo)oxidation are reported in the following.

3.1 - TiO₂ based catalysts

Starting from idea of wet air oxidation (WAO) of NH_3, Taguchi et al. [84] studied the NH_3 decomposition in water solution with O_2 in dark conditions using various kinds of metal-supported catalysts (Pt-TiO$_2$ and Pd-TiO$_2$ among others). They observed that Pd supported on TiO$_2$ also exhibited the ability to oxidize NH_3 to N_2 while Pt–TiO$_2$, under the same conditions, over-oxidized NH_3 to NO_x on the TiO$_2$ surface and NO_2^-/NO_3^- in aqueous solution.

A few years later, Lee et al. [85] observed that the conversion of NH_3 to N_2 was particularly effective over platinized TiO$_2$ under UV illumination when the system was saturated with N_2O. In contrast to biological ammonia conversion which is a two-step process (nitrification/denitrification), the authors suggested that the photocatalytic transformation proceeds in a single step. A key role, discussed later, is played by pH. Indeed, photolysis experiments were carried out at pH 10-11 because ammonium ions do not degrade at all in the UV/TiO$_2$ system. Photocatalytic degradation of ammonia on naked TiO$_2$ is slower and results in its stoichiometric conversion to NO_2^- and NO_3^- without other products. The comparison with Au/TiO$_2$ showed a similar reactivity to undoped TiO$_2$, except that NO_2^- production was higher than that of NO_3^-. Regarding the mechanism, hydrazine might be produced through the dimerisation of the amino radicals ($NH_2\bullet$), but it was not detected and hydroxylamine was produced only at concentrations below the detection limit ($<10\mu M$). The kinetics of ammonia oxidation on metallised TiO$_2$ (for both Au/TiO$_2$ and Pt/TiO$_2$) showed little dependence on whether dioxygen was present. N_2O on Pt/TiO$_2$ produced a dramatically

enhanced effect due to an electron accepting effect. The conversion efficiency of NH_3 to N_2 on Pt/TiO_2 after 2 h irradiation was estimated to be 65-70% in air- or nitrogen- saturated suspensions and over 80% under N_2O saturation. Based upon an electrochemical mechanism proposed by Gerischer and Mauerer [86], similar reaction steps were suggested as a plausible mechanism for the selective photocatalytic conversion of NH_3 to N_2 on Pt/TiO_2. These authors proposed that the active intermediates for dinitrogen formation were NH_x (x = 1,2) species and that the formation of N_{ads} deactivated the electrode surface. The formation of active intermediates NH_x on the naked TiO_2 surface was not favoured. The favourable adsorption of nitrogen species such as NH_3 and NH_x (x = 0,1,2) onto the Pt surface was a prerequisite for the selective photocatalytic oxidation of NH_3 to N_2. The slow adsorption kinetics of ammonia on Pt/TiO_2 implies that the photocatalytic conversion process could be limited by diffusion effects. For the authors the most plausible role of N_2O was the production of OH radicals on Pt/TiO_2. The Pt deposits on TiO_2 enable the selective oxidation of NH_3 to N_2 in two ways: 1) by trapping CB electrons and reductively dissociating N_2O into OH radicals that initiate NH_3 oxidation and 2) by stabilising intermediate NH_x species on Pt and facilitating their recombination to dinitrogen.

Extending the investigation of these catalytic systems, Nemoto et al. [87] found that ammonia can be converted photochemically into H_2/N_2 in a nearly stoichiometric 3:1 ($H_2:N_2$) molar ratio if reacted under alkaline conditions by using $Pt-TiO_2$ and $Pt-SrTiO_3$ suspension. They learn more about the role of the Pt loading and of alkalinity of the feed. At pH 10.7 the evolution of H_2 and N_2 reached a maximum at 0.5wt% Pt, and looks like to be roughly constant between 0.75 and 1.2wt% followed by clear decrease at 2.0 wt% due to the light-shielding effect by the black-coloured Pt loaded on TiO_2. The photochemical reaction yield depends on the number of the irradiated photon, so that if the number of photon is constant, the lower substrate concentration causes higher reaction yield. In suspension systems, it is impossible to measure the intensity of the really absorbed light, so that the quantum yield

could not be determined. Instead of the quantum yield, the reaction yield based on all the incident photons of the monochromatic light (340 nm) was estimated as 5.1%. The lower H_2/N_2 ratio in the initial stage could be ascribed to that the injected e^- would be consumed to occupy the electron trap sites, and hence the amount of H_2 evolution would be lower in the initial stage. The effect of pH on the photodecomposition of NH_3 show that the evolution of H_2 increased steeply at the pH from 9 to 10 showing that the dissociation of NH_4^+ to free NH_3 is important for the photodecomposition (pK_a of NH_3 is 9.24). The evolved H_2 and N_2 decreased over pH 11. In the proposed mechanism the charge separation produces electrons (e^-) and holes (h^+) in the TiO_2 powder resulting in the oxidation of NH_3 by h^+ followed by the reduction of protons on the Pt site. Since the proton concentration in the high pH region is low, the electrons would accumulate in the TiO_2 so that the possibility of recombination between electrons and holes would become high. As a consequence, the oxidation of NH_3 would be suppressed at high pH. It should be also reminded, as previously said, that this selective photocatalytic conversion of ammonia to N_2 is applicable only to NH_3, not to NH_4^+. The effect of some co-catalyst on the photodecomposition show that the RuO_2 cannot work as a H^+ reduction catalyst, since RuO_2 would be reduced by the electrons. In the Pt-$SrTiO_3$ system, the evolved H_2 and N_2 gases were much lower than those obtained with Pt-TiO_2, and the H_2/N_2 ratio (0.64) was very small. The band gap of TiO_2 and $SrTiO_3$ is 3.1 and 3.2 eV, respectively, and the bottom of the conduction band of the latter is slightly more negative than that of the former. For this reason, it is difficult to explain the difference of gas evolution between Pt-TiO_2 and Pt-$SrTiO_3$ by the band structure and redox potential. Therefore, the authors inferred that there is a difference of NH_3 adsorption between two semiconductors, or in the Pt-$SrTiO_3$ system, charge recombination might be easier. Furthermore, a direct excitation of NH_3 caused some complicated and undesired side reactions, so that the evolution of both H_2 and N_2 gases did not occur. Therefore, a Pyrex glass cell to avoid direct excitation of NH_3 or a quartz cell with a non-luminescent glass filter

were adopted to inhibit direct excitation of NH_3. Similar results were obtained over $Pt-TiO_2$ catalysts [83].

S. Shibuya et al. [88] investigated the influence of the pH on the selectivity and rate of the photocatalytic oxidation of ammonia under a flow of air at relatively high NH_3 amount (5–200 mM) to determine the optimum reaction conditions over Pt-loaded TiO_2 to achieve a high oxidation rate and dinitrogen selectivity. The authors showed the time courses of the ammonia, nitrite, and nitrate concentrations as well as the pH during the photocatalytic oxidation of NH_3 at various initial pH. The time course of the concentration of nitrite shows that as it is formed by ammonia oxidation, it is sequentially oxidised to nitrate at pH_i values below 11.3, but its oxidation would be slow at pH_i values above 11.9. The decrease in the oxidation rate above pH 10 is thought to be related to the decrease in ammonia adsorption on the surface of the photocatalyst. At high pH, it is suggested that the hydroxide ion covers the surface of the photocatalyst and prevents the adsorption of ammonia. Complete oxidation of ammonia was achieved when the pH was kept at 10 using Na_2CO_3–$NaHCO_3$ buffer solution.

The influence of the addition of oxygen to the reaction system on the photodecomposition rate of aqueous ammonia on $Pt-TiO_2$ was object of study by S. Shibuya et al. [89]. A possible cause of the increase in the ammonia decomposition rate with the addition of oxygen is the enhancement of the charge separation efficiency. An electron generated by UV irradiation of TiO_2 could easily react with O_2 to give O_2^-, with efficient consumption of the resulting photogenerated electron, thus preventing the accumulation of negative charge on the surface of the photocatalyst [90]. Without oxygen, the photoinduced electron is considered to be consumed by water. This electron consumption step is relatively small and determines the rate of decomposition of ammonia. The main reaction products were nitrate and nitrite

for $[NH_3]_i$ = 5.0 mM under air flow, but the increasing density of N-containing intermediate species on the surface of a photocatalyst affects the selectivity to products.

Microwave heating method was employed by Fuku et al. [91] as a promising technique for the synthesis of Pt–TiO$_2$. The authors observed that the platinum metals on TiO$_2$ cause a positive promoting effect and a negative inhibiting filtering effect of UV light, and these two effects compete in the photocatalytic reaction. The decrease in photocatalytic activity in the presence of a large amount of platinum may be ascribed to the filter effect of the grey-colored platinum loaded on TiO$_2$. The authors also proposed a mechanism: i) the photochemical excitation of a semiconductor material leads to charge separation in the particle, in which electrons e^- are promoted to the conduction band and holes h^+ are left in the valence band; ii) adsorbed NH$_3$ on TiO$_2$ reacts with the generated hole via oxidised intermediates, such as hydrazine and hydroxylamine, to provide N$_2$ and a proton H^+; iii) the electron promoted in conduction band is transported to the platinum metal and then reacts with H^+ to produce H$_2$. Pt acted as a more efficient catalyst for the formation of H$_2$ than Pd by a factor of 2, while the use of Ni and Ag showed negligible activities. This phenomenon is ascribed to the low hydrogen overvoltage of Pt (0.01 V) compared with those of Pd (0.04 V), Ni (0.29 V), and Ag (0.30 V).

Similar results were observed by Kominami [50, 92] studying photo-catalytic decomposition of NH$_3$ and methyl amine in aqueous suspensions of different metal-loaded TiO$_2$ particles. They observed that the decomposition of NH$_3$ occurred easily over Pt-TiO$_2$ compared with water splitting and that NH$_3$ was decomposed to H$_2$ and N$_2$ stoichiometrically without side reactions. The rate was drastically changed depending on the type of co-catalyst, and Pt had the greatest effect as a co-catalyst. The effect as a co-catalyst became smaller with increasing hydrogen over-voltage of the metal when used as an electrode, suggesting that reduction of protons by photogenerated electrons in the conduction band of TiO$_2$ represents

the rate-determining step in this reaction system under the selected operating conditions (in the order: Pt, Pd, Au, Ni, Ag, Cu, Ir). The role of pH observed previously by other researchers was also confirmed. A linear correlation between photocatalytic performance and specific surface area of different TiO_2 samples also was observed, indicating that the surface area of TiO_2 is one of the important factors controlling the photocatalytic activity during H_2 evolution from NH_3 in an aqueous suspension. Finally, rutile samples with Pt exhibited negligible activity due to the location of the conduction band of the rutile phase that is insufficient for the formation of H_2.

The impact of UV and Visible irradiation and specific nitrogen modification on a $5\%Cu/5\%TiO_2/SiO_2$ catalyst for the oxidation of ammonia were studied by Kowalczyk et al. [93]. The authors demonstrated that both UV and Vis irradiation increased the conversion of the reactant. Higher ammonia conversion was achieved due to a good distribution of titanium dioxide and copper on the surface of the support.

Catalysts in aqueous suspension based on Pt, Pd, Au and Ag nanoparticles (NPs) deposition on TiO_2 were studied by Altomare et al. [94]. Apart from Au-modified TiO_2, the metal NPs-containing photocatalysts clearly exhibited a higher photoactivity in ammonia oxidation with respect to naked P25 titania and to the blank sample due to a more effective separation of the photoproduced electron-hole couples induced by the presence of metal NPs, working as electron traps on the photocatalyst surface [95]. The rate of ammonia photocatalytic oxidation followed the trend 1Ag > 1Pt > 1Pd > P25 > 1Au, which was also paralleled by an increase of selectivity to NO_3^-. Ammonia photo-oxidation up to nitrate ions was shown to occur through a series of consecutive reactions, nitrite anions being the intermediate species detected during the runs [96]. These results clearly highlight that the type of metal NPs deposited on titania affect ammonia conversion and products selectivity, suggesting that different photocatalytic paths may prevail in the presence of different noble

metal NPs on TiO_2. One may thus conclude that with Pd- and Au-containing photocatalysts ammonia photo-conversion into nitrate anions occurs in a single, complete oxidation step on the photocatalyst surface, without the formation of any intermediate species detectable in the aqueous phase. N_2 evolution takes place through a path parallel to the main oxidation route, occurring through a series of chain reactions directly involving ammonia in activated form. Species which have been hypothesised to form upon ammonia direct or indirect interaction with photoproduced holes on the photocatalyst surface include hydrazine and/or hydroxylamine. NPs of different metals on the TiO_2 surface, as well as different metal loadings, favour different ammonia photo-oxidation paths on the semiconductor surface. These depend also on the intermediate species produced on the photocatalyst surface, containing nitrogen in different oxidation states, which combine or disproportionate on the activated surface. Indeed, metal NPs not only act as mere electron-traps, thus making the photoproduced holes more prone to ammonia oxidation, but may also affect the mechanism of ammonia oxidation itself, by interacting and/or stabilising the photo-activated and intermediate species in different ways.

Obata et al. [97] observed that the photocatalytic activity of ammonia photodecomposition was increased when TiO_2 was doped with Fe ($Pt/Fe–TiO_2$), while the photocatalyst doped with Cr ($Pt/Cr–TiO_2$) showed almost similar photocatalytic activity as Pt/TiO_2. It is reported that when Cr^{3+} ions are partly substituted for Ti^{4+} ions in TiO_2, oxygen defects and/or Cr^{6+} ions are formed to keep the charge balance. Cr^{6+} ions may play a role in the recombination centres between photogenerated electrons and holes. It is thus suggested that the $Pt/Cr–TiO_2$ photocatalyst deactivated in comparison with $Pt/Fe–TiO_2$ photocatalyst. Using the $Pt/Fe–TiO_2$ photocatalyst the photodecomposition of NH_3 in D_2O solution did not cause the formation of D_2, but the formation of H_2. Hence, hydrogen formation is established as being derived from the photodecomposition of ammonia. The Fe dopant can be inserted into the TiO_2 lattice as a Fe impurity levels below the conduction band and above the valence band

of TiO_2, creating an optical band gap. Therefore, it is speculated that the substitution of Ti^{4+} with Fe^{3+} in $Fe–TiO_2$ leads to the more effective utilisation of irradiated light.

Reli et al. [98] used cerium-doped TiO_2 prepared by the sol–gel method for the photocatalytic decomposition of ammonia because the addition of cerium lowers the band gap of the photocatalyst. The effect of irradiation time on the formation of hydrogen in the photocatalytic decomposition of ammonia was investigated over TiO_2 as well as over TiO_2 photocatalysts loaded with different amount of cerium over a period of 0–10h. The addition of cerium led to positive increase of specific surface area and also to a favourable decrease of band gap. For the ammonia photocatalytic decomposition, the energy of electron formation in conduction band must be higher than N_2/NH_4OH reduction potential and the hole energy in valence band must be lower than OH^- oxidation potentials. The addition of Ce to TiO_2 should result in changing the band gap and the absorption edge energies and it can be concluded that for 1.2 wt.% Ce/TiO_2 photocatalyst have the most favourable potentials for the photocatalytic decomposition of ammonia. The authors also compared the hydrogen yields after 6 h of irradiation over 1.2 wt.% Ce/TiO_2, 2.7 wt.% Pt/TiO_2, ZrO_2 and ZnO photocatalyst [99].

Yuzawa et al. [100] investigated the photocatalytic ammonia decomposition of both gaseous and aqueous ammonia on metal loaded titanium oxide in detail, and successfully clarified the mechanism. About the support, they observed that the junction between anatase and rutile phases would enhance the charge separation [101, 102] and that the photocatalytic activity of rutile was generally lower than that of anatase [103]. The metal having larger work function, *i.e.* lower Fermi level, was effective for the gaseous ammonia decomposition, thus platinum better promoted the reaction. Moreover, the work function of bulk metal correlated linearly with the logarithm of the hydrogen production rate, suggesting that photocatalytic

activity would be mainly derived from the charge separation ability for the photoformed hole and electron pair [104].

In the spectral region around 385 nm, the production rate was slightly higher than the corresponding light absorption. This region of light can contribute to the activation of ammonia chemisorbed on the surface Ti site of titanium oxide, in absence of water, through the excitation from the N 2p orbital of ammonia to the Ti 3d orbital [105]. The authors confirmed that the reaction rate of the photocatalytic decomposition of NH_3 was much higher than that of the photocatalytic decomposition of NH_4^+. The dominant reactant is confirmed NH_3, according to Zhu *et al.* [77] and consistent with the fact that ammonium ion was an inactive species for oxidation by hydroxyl radical ($\cdot OH$), which is one of the strongest oxidants. ESR spectra of adsorbed ammonia before and upon photoirradiation showed that the signal intensity of Ti^{3+} increased. Excess formation of Ti^{3+} would result in the release of lattice oxygen from titania and the formation of a colour centre, which would be the reason for the colour change of titanium oxide. Surface amide radical was also observed. These results suggest that the amide radical would be the dominant active species produced from NH_3 through the reaction with the photogenerated hole or surface hydroxyl radical. Platinum nanoparticles efficiently received the electron from the conduction band of the TiO_2. The amide radical as the first intermediate would form hydrazine over platinum loaded titanium oxide. It is known that the disproportionation into hydrazine and nitrogen and self-decomposition into hydrogen and nitrogen can proceed very easily under ambient temperature and pressure. Water would be important to promote the photocatalytic cycles for a long time. Finally, the authors propose a mechanism in gaseous phase and wet conditions.

Kinetic modeling was carried out for the photocatalytic oxidation of ammonia and nitrites [106]. The authors compared the initial rates of both reactions as a function of pH in order

to validate the hypothesis that the rate controlling step was the adsorption of the reactants. Adsorption depends on surface charge which is in turn determined by pH for a given semiconductor. Positively charged surfaces should inhibit ammonium adsorption, but excessively high pH would shift the acid base equilibrium towards ammonia, with lower effect of surface charge on adsorption. Thus ammonium adsorption can be favoured at pH comprised between the isoelectric point of the semiconductor and the pK_a of the species to be adsorbed and reacted. Similar electrostatic effects were observed for NO_2^- photooxidation. The two reactions seem to occur independently. This may suggest that the adsorption sites are different, without competition. At difference with very simple kinetic models usually proposed for photocatalysis, a Langmuir-Hinshelwood approach was suggested by the authors to take into account adsorption.

The effects of the TiO_2 crystal structure (rutile, anatase and brookite) in the photocatalytic oxidation of NH_3 was studied [107]. Among the different photocatalysts investigated in the present study, pure brookite appears to have maximum beneficial effect on photo-activity from Pt NPs deposition, especially if carried out by the modified deposition-precipitation method employed in the cited work.

D. Sun et al. [108] studied the photocatalytic removal of aqueous NH_4^+/NH_3 by $TiO_{2-x}N_x/PdO$ nanoparticles. NH_4^+/NH_3 removal over 90% could be achieved under visible light illumination and the production of toxic photocatalytic oxidation by-products (NO_3^- and NO_2^-) was minimised. $TiO_{2-x}N_x/PdO$ nanoparticles were synthesised by a sol–gel process at room temperature. The photocatalytic removal of aqueous NH_4^+/NH_3 under visible light illumination was also dependent on the initial solution pH. With the increase of $TiO_{2-x}N_x/PdO$ amount, the aqueous ammonia removal ratio firstly increased and then gradually decreased. When the photocatalyst concentration was too low, the production of reactive oxygen species was limited, affecting its photocatalytic performance. When the concentration was

too high, the light transmittance in the solution could be affected and its light energy utilisation would subsequently be hampered, also limiting the photo-catalytic performance. With the increase of the irradiation intensity, the aqueous ammonia removal ratio firstly increased and then decreased. The observed decrease of the photocatalytic performance under intense visible light illumination could be attributed to the changes in the chemical status of PdO after intense visible light illumination. Indeed, part of PdO could be reduced to Pd, and Pd could be gradually oxidised back to PdO, to return to the original state. Thus, the optimised reaction conditions for catalyst nano-particles were determined with the initial solution pH at 10, the photocatalyst amount at 0.4 g/L, and the visible light illumination intensity at 100 mW/cm^2. PdO nanoparticles could serve as the trapping centres for photo-generated electrons, beneficial to the separation of e$^-$/h$^+$ pairs. Thus, the lifetime of holes could be largely increased during the photocatalytic process, which induced a largely enhanced photocatalytic oxidation performance under visible light illumination.

A prototype of photo-reactor was also proposed [96], in which farms manure can directly be treated to decrease its nitrogen content before using it as a field fertiliser. Experiments, carried out by irradiating ammonia solutions with UV-A light in the absence of TiO_2 powder, excluded that direct NH_3 photolysis took place under the mild irradiation conditions. Negligible ammonia adsorption occurred in the dark on TiO_2 at pH 10.5. This is expected, because ammonia is prevalently in its neutral form at this pH, whereas the semiconductor surface is negatively charged, its point of zero charge being around 6.25 [109]. The rate of ammonia photocatalytic abatement was correlated to the concentration of O_2 dissolved in the reaction medium, confirming that dissolved O_2 plays a significant role. In fact, photopromoted electrons easily react with O_2 to give $O_2^-\bullet$, with the resulting consumption of conduction band electrons. This would partially suppress the undesired recombination of photo-produced electron and hole couples, indirectly enhancing the rate of ammonia oxidation by the holes or by the hydroxyl radicals generated through electron transfer from

water or hydroxyl anions to the photo-generated holes. As frequently found in photocatalysis, the percent conversion of the ammonia substrate decreased with increasing initial $[N]_i$ from 100 to 1000 ppm. Conversely, the selectivity to N_2 increased with increasing the initial substrate concentration, possibly as a consequence of an increased probability of N_2 production resulting from redox reactions involving ammonia and the photocatalytically produced species containing nitrogen in different oxidation states and adsorbed on the photocatalyst surface. At pH higher than 10.5, a rate decrease was observed, probably due to competitive adsorption of hydroxide anions on the photocatalyst surface. The hindered photo-oxidation of nitrite to nitrate ions should also be attributed to this effect, as observed under extremely alkaline conditions. Conversely, under slightly acidic conditions, *i.e.* at pH ~ 6.5 the rate of nitrite photo-oxidation to nitrate was much higher. P25 TiO_2 showed the highest photocatalytic activity among all of the investigated titania samples, together with a good selectivity to N_2. The high ammonia conversion can be attributed to a decreased recombination rate of the valence band holes h_{VB}^+ with conduction band electrons e_{CB}^- for TiO_2 containing both anatase and rutile phases [76, 110]. With the only exception of P25, exhibiting high photoactivity with a relatively small surface area, the photo-activity generally increased with increasing the photocatalyst surface area. All anatase samples showed higher photoactivity compared to rutile samples, as already found for other photocatalytic reactions. Authors concluded that during the photocatalytic treatment ammonia was either mildly oxidised to N_2 or transformed into oxidised nitrogen-containing species persisting in the aqueous phase, *i.e.* nitrite and nitrate anions. The co-presence of ammonia and of its oxidation intermediates seems to play a crucial role in conversion of N-containing pollutants into innocuous N_2. Finally, the authors reported that both solid residua in manure and other bio-organic substances undergoing mineralisation affected the photocatalytic performance in the prototype reactor.

The effect of inorganic anions (Cl^-, SO_4^{2-}, $HPO_4^{2-}/H_2PO_4^-$, and HCO_3^-/CO_3^{2-}) usually present in water and/or wastewaters on the photocatalytic oxidation of NH_4^+/NH_3 to NO_2^- by H_2O_2 over TiO_2 as a function of pH was studied by Zhu et al. [111]. The different reaction rate was due to either (i) different rates of •OH scavenging by Cl^-, SO_4^{2-}, HPO_4^{2-}, HCO_3^-/CO_3^{2-}, according to [112], and/or (ii) different rates of direct oxidation of NH_4^+/NH_3 by the corresponding anion radicals, with the fastest rate of direct oxidation by $HPO4^{•-}$. CO_3^{2-} is a better •OH scavenger with respect to Cl^-, SO_4^{2-}, or HPO_4^{2-}, inhibiting NH_4^+/NH_3 oxidation. Adsorption of HPO_4^{2-} enhanced the initial rate of NH_4^+/NH_3 photocatalytic oxidation because adsorption of HPO_4^{2-} increased the negative charge of the TiO_2 surface, leading to neutralisation of NH_4^+ to NH_3 on the TiO_2 surface. The authors concluded that photocatalytic oxidation of NH_4^+/NH_3 to NO_2^- is the rate-limiting step in the complete oxidation to NO_3^- in the presence of common wastewater anions.

The feasibility of using TiO_2 photocatalysis to recycle grey water, containing aqueous ammonia and synthetic surfactants, for reuse was studied by Zhu et al. [113]. Surfactants and monosaccharides would decrease the photocatalytic degradation rate of NH_4^+/NH_3 by: (a) competitive adsorption of surfactants with NH_4^+/NH_3 for TiO_2 surface sites and/or (b) formation of byproducts that would serve as •OH scavengers. Consistently with previous studies, NO_2^- and NO_3^- were the major products. Initial rates of NH^{4+}/NH_3 degradation, however, were slowered by surfactants. Adsorption of surfactants over TiO_2 showed no relationship between TiO_2 surface coverage and the decrease of initial rates of NH_4^+/NH_3 removal. The authors modified the experimental conditions to facilitate the estimation of the concentration of •OH and they observed that the formation of •OH scavengers was the main reason for decreasing the initial rates of NH_4^+/NH_3 degradation in the presence of surfactants or monosaccharides. They moreover observed that CO_3^{2-} was probably more important as a radical scavenger than HCO_3^- under the selected experimental conditions.

Using a Pt/TiO_2 suspension may not in general be economical as a practical water treatment technology because catalyst immobilisation or recovery processes should be considered for practical applications. Utilisation of deposited titania is desirable because it precludes the need for post-use filtration to remove the photocatalyst. This aspect was treated by Pretzer et al. [114], reporting that titania–acrylic composite materials showed sufficient titania adhesion strength to facilitate the long-term durability needed for aqueous applications. The presence of the intermediate NH_x and NH_2OH species in the production of N_2 and NO_3^-, respectively, were important differentiators between different reaction mechanisms proposed. Therefore, a determining factor for selectivity to N_2 was the formation and stabilisation of these species. As already pointed out, excessive presence of Pt resulted in a decrease in k_{dec} and k_{ox} because Pt oxides have an inhibiting effect on the oxidation rate and selectivity of titania-catalysed ammonia oxidation due to their inability to stabilise intermediate NH_x species and their role as recombination centres for electron–hole pairs via the cyclic oxidation and reduction of Pt^{2+} and Pt^{4+}. Recombination of electron–hole pairs inhibits the desired redox reaction by limiting the concentration of hydroxyl radicals produced. This reduction in the production of hydroxyl radicals not only depresses the reaction rate, but may also have an effect on the selectivity. The proposed mechanism for nitrate production via ammonia oxidation is depicted in path 2, whereas that resulting in nitrogen gas is reported in path 1, which evidence the effect of the hydroxyl radicals on selectivity [114].

Path 1:

$$NH_3 + {}^\bullet OH \rightarrow NH_2 + H_2O \qquad\qquad 19)$$

$$NH_2 + {}^\bullet OH \rightarrow NH + H_2O \qquad\qquad 20)$$

$$NH + {}^\bullet OH \rightarrow N + H_2O \qquad\qquad 21)$$

$$NH_x + NH_y \rightarrow N_2H_{x+y} \quad (x,y= 0,1, 2) \qquad 22)$$

$$N_2H_{x+y} + (x+y) \, h^+ \rightarrow N_2 + (x+y)H^+ \qquad 23)$$

Path 2:

$$NH_3 + {}^{\bullet}OH \rightarrow HONH_2 + H^+ \qquad 24)$$

$$HONH_2 + {}^{\bullet}OH \rightarrow NO_2^- \rightarrow NO_3^- \qquad 25)$$
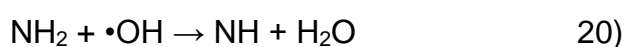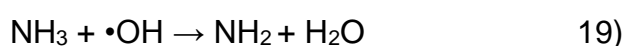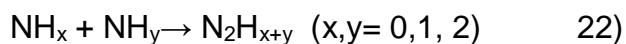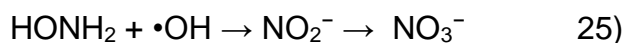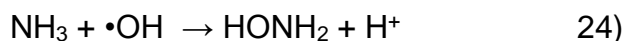
An additional determining factor in the production of nitrogen gas is the formation and stabilisation of NH_x species. It has been noticed that Pt^0 is able to stabilise such intermediates, thereby favouring the production of N_2. Pt can be increasingly reduced as some of the electrons donated by the oxidised species are utilised for the reduction of Pt in addition to the more dominant reduction of the hydroxyl radicals present. An increase in the amount of reduced Pt occurred particularly for Pt concentrations between 3% (w/w) and 4% (w/w) after exposure to a Poly-Oxometallate (phosphotungstic acid). The neutral pH indicates that the required ammoniacal species for the photocatalytic oxidation of ammonia with titania is NH_3. Again, this difference in reactivity is likely due to the enhanced interaction strength of ammonia with titania as compared to ammonium.

The photoxidation of NH_3/NH_4^+ to nitrite/nitrate using microwave-induced Titania Nano Tubes (TNTs) Ou et al. [115] and platinised TNTs Ou et al. [116] has been studied. Partly intercalated NH_3/NH_4^+ within TNTs could be transformed to NO_2^- and NO_3^-, indicating an alternative pathway in forming NO_2^- and NO_3^- besides the common photocatalytic oxidation of aqueous NH_3/NH_4^+. The kinetics follow a simple first-order model. The light-shielding effect (filter effect), due to catalyst overloading was not apparent when NH_4^+ was intercalated into the zig-zag structure of TNTs. The selective formation of N_2 during NH_3/NH_4^+

photoxidation was likely enhanced as well, since the specific adsorption of precursors (NH_3 and NH_x) on Pt was a prerequisite for N_2 formation. The over-oxidation of NH_3/NH_4^+ to NO_2^- was sensitive to an optimal Pt loading. However, the effect of Pt content on N_2 recovery did not follow the same trend as the recoveries of NO_2^-/NO_3^-. This was interpreted in terms of NH_3 adsorbed on the metallic Pt as a prerequisite step leading to N_2 formation. In contrast, NO_2^- was formed primarily from NH_3 adsorbed on the non-platinised TNT sites. N_2 formation during photocatalytic oxidation of NH_3/NH_4^+ was exclusively formed from the selective oxidation of NH_3/NH_4^+. A kinetic equation with parallel and consecutive reactions was proposed to describe the kinetics of NH_3/NH_4^+ photoxidation over platinised TNTs. In contrast to the common Pt-TiO_2 catalysts, PtO_2 supported on platinised TNTs presented no negative effect on the performance of NH_3/NH_4^+ photoxidation. The authors suggested a plausible mechanism and conceptual reaction pathway for NH_3/NH_4^+ photoxidation over such catalytic systems.

Shavisi et al. [117] studied the influence of solar light irradiation on ammonia degradation from petrochemical industry wastewater using TiO_2/LECA (Light Expanded Clay Aggregate) photocatalyst easily separable from the suspension after cleaning up the wastewater. The degradation efficiency in the presence of solar light was lower than UV irradiation, since TiO_2/LECA photocatalyst was mainly photoactive under UV light. Data indicate that the difference between solar efficiency and UV was 15.9%. The increased amount of catalyst up to 25 g/L increased the quantity of photons absorbed and consequently the degradation rate. The decreased degradation rate at higher catalyst loading (higher than 25 g/L of TiO_2) may be due to deactivation by collision of ammonia and other molecules or deactivated due to the formation of a dense layer of catalysts. Increase of pH from 3 to 11 increased the ammonia conversion from 46.2 to 96.5%, whereas 11 to 12, the removal efficiency was decreased. The authors suggested that the degradation experiments by UV irradiation and solar light of ammonia followed a Langmuir–Hinshelwood kinetics and observed that when

the TiO$_2$/LECA photocatalyst stayed in wastewater for a long time, the pollutant molecules adsorbed on the surface of the photocatalyst. Thus, to remove these compounds from the catalyst surface, a four-stage process was needed.

Rongé et al. [118] described the influence of TiO$_2$ Layer-by-layer (LbL) deposition parameters on resulting film structure, and its corresponding photocatalytic activity in ammonia degradation.

3.2 - Other photocatalysts

To create a new visible light photocatalyst Kaneko et al. [119] proposed a photocatalytic system using a dye-sensitised system, composed of a sensitiser (Ru(bpy)$_3^{2+}$), an electron mediator (methylviologen) and an electron-acceptor (O$_2$). The irradiation of the aqueous solution of NH$_3$ and Ru(bpy)$_3^{2+}$ by visible light in the presence of K$_2$S$_2$O$_8$ induced the formation of Ru(bpy)$_3^{3+}$ by oxidation of the photoexcited Ru. Methylviologen works as an acceptor from the photoexcited Ru complex in place of K$_2$S$_2$O$_8$ to produce the viologen cation radical. N$_2$ was formed after an induction period as desired product.

Sun *et al.* [120] reported the photodegradation of NH$_4^+$/NH$_3$ and phenol in aqueous solution by "flower-like" Bi$_2$Fe$_4$O$_9$, hydrothermally synthesised with the assistance of an ambient magnetic field, with visible light. 32% of the NH$_4^+$/NH$_3$ was degraded after 6h in the presence of bulk-Bi$_2$Fe$_4$O$_9$, indicating the excellent photocatalytic performance. Theoretical calculations indicate that the Bi$_2$Fe$_4$O$_9$ was a multiband semiconductor. The middle band may act as recombination centres, which indicates that efficient electron-hole separation principally helps the improvement of photocatalytic performance of this catalytic system.

Wang et al. [121] consider that metals are relatively expensive materials with limited resources, and thus alternative photocatalysts based on precious-metal-free materials

should be actively pursued. They seek to explore the photocatalytic ability of atomic single layer (SL) g-C_3N_4 for aqueous ammonia treatment under Xe lamp irradiation. Total ammonia nitrogen (TAN) decreased significantly under irradiation, demonstrating a good photocatalytic activity for ammonia treatment. The performance of SL g-C_3N_4 was also evaluated in the visible light region. Although the TAN decrease tendency was lower than that of under the full output of Xe lamp irradiation, the TAN concentration also continually decreased with time under visible light irradiation. A suitable concentration of SL g-C_3N_4 was crucial for optimising the photocatalytic reaction because large amount of photocatalysts could induce a significant decrease of light penetration. The SL g-C_3N_4 exhibited more effective photocatalytic activity in alkaline solution than in neutral or acidic solutions. With decreasing TAN concentration, other inorganic nitrogen forms appeared. The stability of SL g-C_3N_4 was also evaluated. •OH was the dominant reactive radical species for ammonia oxidation, but the photogenerated holes in the catalyst could not oxidise hydroxyl ion (OH^-) to form •OH because the standard redox potential of g-C_3N_4 was more negative than the standard redox potentials of •OH/OH^-; so the authors suggested that •OH may form through the photogenerated electrons from the conduction band of g-C_3N_4 and the possible pathways for ammonia photocatalytic oxidation to nitrite and nitrate might involve a direct oxidation process induced by the photogenerated holes and/or by the oxidation of •OH that formed from the photogenerated electrons.

Bo et al. [122] presented the activated carbon (AC)-nickel ferrite as a hybrid catalyst for the photo-Fenton oxidation of ammonia in the presence of hydrogen peroxide under visible light irradiation. AC-$NiFe_2O_4$ catalyst was capable of responding to visible light and the activated carbon played an indispensable role in absorbing visible light. The optimal mass concentration of AC was equal to 4.0% in the composite catalyst for the degradation of ammonia. The oxidation pathway for ammonia went through the hydrazine intermediate to form nitrite ions. The kinetic studies showed that the oxidation of ammonia followed a

pseudo-first order kinetic law. The authors showed that the activated carbon played the role in absorbing photons, forming photo-generated electrons and transferring the photo-generated electrons to the Fe 3d orbital.

Zhang *et al.* [123] studied Bi_2WO_6 nanoplates prepared by the hydrothermal method for ammonia oxidation under the irradiation of a household fluorescent lamp. Photocatalytic oxidation reaction was carried out in the presence of radical scavengers: superoxide dismutase (SOD) and triethanolamine (TEOA) as trap for holes photogenerated in the catalyst. Bi_2WO_6 oxidised predominantly NH_4^+/NH_3 into NO_2^- and NO_3^-. The reaction rate increased when raising the pH in the range 9.3–11.2. The high initial concentration of the pollutant and complex ingredient result in increased irradiation time for full ammonia oxidation. The photogenerated holes of the Bi_2WO_6 nanoplates are involved in the photocatalytic oxidation process of the ammonia as detailed in the proposed reaction mechanism.

Finally, Zhou et al. [124] prepared via a hydrothermal method a graphene-manganese ferrite hybrid catalyst and evaluated its photo-Fenton catalytic activities during NH_3 decomposition under visible light irradiation in the presence of hydrogen peroxide. The rG–$MnFe_2O_4$ hybrid photo-Fenton catalyst can degrade NH_3 effectively into N_2 under visible light irradiation. Stability tests demonstrated that the proposed catalytic system was highly stable and easily separable and recyclable. The proposed mechanism hypothesises that Mn and Fe act simultaneously during the oxidative NH_3 degradation.

3.3 - Photoelectrocatalytic systems

Kaneko et al. [125] presented a simple nanoporous TiO_2 film coated on a glass substrate highly active and concluded that the nanoporous TiO_2 formed a sort of Schottky junction

(called a liquid-junction) with aqueous ammonia. Then the authors consider a liquid-junction n-semiconductor photoelectrochemical system, where excitation of electrons from the valence band takes place by irradiation of the semiconductor with proper wavelength. This process forms separated electrons (in the conduction band) and holes (in the valence band) and thus separated charges can promote oxidation and reduction reactions at the photoanode and the cathode. Since the photocurrent increased at first sharply and reached rapidly an equilibrium state, most of the separated electrons must be transported to the cathode due to the band bending rather than escaping directly outside the nanostructured TiO_2 reducing O_2 there. The same authors studied also the effect of the cell structure composed of a TiO_2 photoanode and an O_2-reducing cathode and the photodecomposition of ammonia in terms of quantum efficiency.

Nemoto et al. [87] investigated the effect of Pt loading on TiO_2/FTO (Fluorine doped Tin Oxide) nanoporous film. In the case of using TiO_2/FTO as a photoanode and Pt as a cathode, the NH_3 photodecomposition took place stoichiometrically. On the contrary, the same reaction did not easily occur in the case of using Pt-TiO_2/FTO as a photoanode. In the former case the oxidation and reduction take place on the anode and on the cathode, respectively. On the other hand, both oxidation site (TiO_2) and reduction site (Pt) coexisted in the same photoanode, which would make the photodecomposition difficult, although the Pt-TiO_2/FTO should work as a photocatalyst by itself for the NH_3 decomposition without Pt cathode. The authors propose a mechanism of the NH_3 photodecomposition by irradiation on TiO_2 photoanode extended to NH_3 photodecomposition:

$$TiO_2 + hv \rightarrow e^- + h^+ \hspace{3cm} 26)$$

$$2\ NH_{3ads} + 6\ h^+ \rightarrow 2\ (NH_3)_{ox} \rightarrow N_2 + 6\ H^+ \hspace{1.5cm} 27)$$

$$e^- + Pt \rightarrow Pt(e^-) \hspace{3cm} 28)$$

$$6 \, H^+ + 6 \, Pt(e^-) \rightarrow 3 \, H_2 + 6 \, Pt \qquad\qquad 29)$$

$$2 \, NH_3 \rightarrow N_2 + 3 \, H_2 \qquad\qquad 30)$$
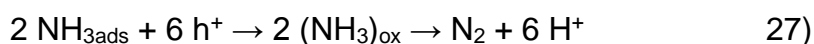
The structure of the $(NH_3)_{ox}$ was not determined specifically, but a possible candidate could be hydrazine or hydroxylamine. Since free NH_3 is mainly active for the photodecomposition, the electron donation from the lone pair of the NH_3 to the electron-deficient TiO_2 site would be principally of importance rather than NH_3 adsorption onto titania, which should be much more favourable for NH_4^+ than for the free NH_3.

To summarise, some of the reported examples of ammonia photodecomposition or photooxidation are collected in Table 3.

Table 3: Examples of ammonia photodecomposition or photooxidation processes.

Catalyst	Co-catalyst	Conversion NH_3/NH_4^+ (%)	Selectivity N_2 (%)	Reference
TiO_2	Pt, Ru, Pd, Rh, Cu, Co, Ni	100	100	84
TiO_2	Pt, Au	100	ca. 80	85
TiO_2	Pt	-	-	87
TiO_2	Pt	100	NO_x^-	88,89
TiO_2	Pt	-	-	91
TiO_2	Pt, Pd, Au, Ag, Cu, Ir, NiO	-	-	92
TiO_2/SiO_2	Cu	100	-	93
TiO_2	Pt, Pd, Au, Ag	Max. 45	Max. 40	94
TiO_2, ZnO	Ce	Report H_2 yield / production rate		98, 99
TiO_2	Pt, Rh, Pd, Au, Ni, Cu	Report $H_2 + N_2$ production rate		100
TiO_2	-	93	NO_x^-	106
TiO_2	Pt	51	27	107

$TiO_{2-x}N_x$	PdO	80	-	108
TiO_2	-	Ca. 70%	-	113
TiO_2	Pt	100	NO_x^-	114
$Na_xH_{2-x}Ti_3O_7$	-	53	NO_x^-	115
Titanate nanotubes	Pt	Ca. 70	87.5	116
$Ru(bpy)_3^{2+}$	-	N_2 formation rate		119
$Bi_2Fe_4O_9$	-	70	-	120
$g-C_3N_4$	-	80	NO_x^-	121
AC - $NiFe_2O_4$	-	90	NO_2^-	122
Bi_2WO_6	-	100	NO_3^-	123
$rG–MnFe_2O_4$	-	90	-	124
TiO_2		70	Ca. 100	125

4 – Conclusions

The abatement of N-containing inorganic pollutants from waste and drinking water is a challenging task, due to the toxicity (acute and chronical) of the compounds considered and to the poor effectiveness and criticisms of the present depuration technologies on this point. The photocatalytic abatement of nitrate, nitrite and ammonia has been investigated to a lower extent with respect to other processes for water treatment (*e.g.* the removal of organic contaminants). In spite of this, interesting results in terms of conversion of the reactant have been achieved with metal-doped TiO_2. The reactions can occur under mild conditions, but require special attention to improve the lifetime of the photogenerated charges. For this reason, usually metals are deposed over the photocatalyst as electron sinks and easily oxidisable molecules are used as hole scavengers. This improved very much the photoreactivity. A special attention should be put in the selection of the proper pH, which is mainly found important to determine the adsorption of reactants (and intermediates) over the catalyst surface.

Despite these attempts to accomplish full NO_x^- or NH_3 conversion, the unsolved key point remains catalyst/process selectivity to N_2. This is in most cases unsatisfactory or not suitably determined during testing both for the photooxidation/decomposition of ammonia and for the photoreduction of nitrates and nitrites. Indeed most papers report calculated N_2 selectivity by difference from other determined species.

In any case, the research seems limited to a bench scale application, with only few papers addressing important issues for the practical implementation, such as photoreactor design, transport properties, catalyst immobilisation, the effect of real substrates, etc.

Acknowledgements

References

1.   K. R. Burow, B. T. Nolan, M. G. Rupert, and N. M. Dubrovsky, *Environ. Sci. Technol.* 44, 4988 (2010).
2.   B. T. Nolan, L. J. Puckett, L. W. Ma, C. T. Green, E. . Bayless, and R. W. Malone, *J. Environ. Qual.* 39, 1051 (2010).
3.   J. Lee, H. Park, and W. Choi, *Environ. Sci. Technol* 36, 5462 (2002).
4.   M. H. Christensen and P. Harremoes, *Wat. Pollut. Microbiol.* 2, 391 (1978).
5.   B. G. Volkmer, B. Ernst, J. Simon, R. Kuefer, G. J. Bartsch, D. Bach, and J. E. Gschwend, *BJU. Int* 95, 972 (2005).
6.   H. epa. gov/iris/subst/0076. ht. U.S. Environmental Protection Agency. 1991. "Integrated Risk Information System (IRIS): Nitrate."
7.   J. Bukowski, G. Somers, and J. Bryanton, *J. Occup. Environ. Med* 43, 377 (2001).
8.   L. George, M. Wiklund, M. Aastrup, J. Pousette, B. Thunholm, T. Saldeen, L.

Wernroth, B. Zaren, and L. Holmberg, *Eur. J. Clin. Invest.* 31, 1083 (2001).

9. M. I. Cedergren, A. J. Selbing, and B. A. Källén, *Environ. Res* 89, 124 (2002).

10. J. D. Brender, J. M. Olive, M. Felkner, L. Suarez, W. Marckwardt, and K. A. Hendricks, *Epidemiology* 15, 330 (2004).

11. http://water.epa.gov/scitech/swguidance/standards/criteria/aqlife/ammonia/

12. www.who.int

13. M. Shand and J. a. Anderson, *Catal. Sci. Technol.* 3, 879 (2013).

14. M. S. Kim, S. H. Chung, C. J. Yoo, M. S. Lee, I. H. Cho, D. W. Lee, and K. Y. Lee, *Appl. Catal. B Environ.* 142-143, 354 (2013).

15. N. Barrabés and J. Sá, *Appl. Catal. B* 104, 1 (2011).

16. I. Mikami, Y. Sakamoto, Y. Yoshinaga, and T. Okuhara, *Appl. Catal. B* 44, 79 (2003).

17. A. Aristizábal, S. Contreras, N. Barrabés, J. Llorca, D. Tichit, and F. Medina, *Appl. Catal. B* 110, 58 (2011).

18. M. Halmann and K. Zuckerman, *J. Chem. Soc., Chem. Commun.* 455 (1986).

19. A. Pandikumar, S. Manonmani, and R. Ramaraj, *Catal. Sci. Technol.* 2, 345 (2012).

20. Y. Li and F. Wasgestian, *J. Photochem. Photobiol. A Chem.* 112, 255 (1998).

21. K. T. Ranjit, R. Krishnamoorthy, T. K. Varadarajan, and B. Viswanathan, *J. Photochem. Photobiol. A Chem.* 86, 185 (1995).

22. K. T. Ranjit and B. Viswanathan, *J. Photochem. Photobiol. A Chem.* 108, 73 (1997).

23. K. T. Ranjit and B. Viswanathan, *J. Photochem. Photobiol. A Chem.* 107, 215 (1997).

24. T. Yang, K. Doudrick, and P. Westerhoff, *Water Res.* 47, 1299 (2013).

25. H. Gekko, K. Hashimoto, and H. Kominami, *Phys. Chem. Chem. Phys.* 14, 7965 (2012).

26. H. Kominami, H. Gekko, and K. Hashimoto, *Phys. Chem. Chem. Phys.* 12, 15423 (2010).

27. L. F. Liu, Y. Zhang, F. L. Yang, G. Chen, and J. C. Yu, *Sep. Purif. Technol.* 67, 244 (2009).

28. F. Zhang, Y. Pi, J. Cui, Y. Yang, X. Zhang, and N. Guan, *J. Phys. Chem. C* 111, 3756 (2007).

29. B. Ohtani, M. Kakimoto, H. Miyadzu, S. Nishimoto, and T. Kagiya, *J. Phys. Chem.* 92, 5773 (1988).

30. F. Zhang, R. Jin, J. Chen, C. Shao, W. Gao, L. Li, and N. Guan, *J. Catal.* 232, 424 (2005).

31. K. Doudrick, T. Yang, K. Hristovski, and P. Westerhoff, *Appl. Catal. B Environ.* 136-137, 40 (2013).

32. A. Sowmya and S. Meenakshi, *J. Water Process Eng.* 8, e23 (2015).

33. M. D'Arienzo, J. Carbajo, A. Bahamonde, M. Crippa, S. Polizzi, R. Scotti, L. Wahba, and F. Morazzoni, *J. Am. Chem. Soc.* 133, 17652 (2011).

34. M. K. Nowotny, L. R. Sheppard, T. Bak, and J. Nowotny, *J. Phys. Chem. C* 112, 5275 (2008).

35. H. Z. Cheng and A. Selloni, *Phys. Rev. B* 79, 92101 (2009).

36. D. Sun, W. Yang, L. Zhou, W. Sun, Q. Li, and J. K. Shang, *Appl. Catal. B Environ.* 182, 85 (2016).

37. a. V. Lozovskii, I. V. Stolyarova, R. V. Prikhod'ko, and V. V. Goncharuk, *J. Water Chem. Technol.* 31, 360 (2010).

38. D. M. Stanbury, *Adv. Inorg. Chem.* 33, 69 (1989).

39. T. Mishra, M. Mahato, N. Aman, J. N. Patel, and R. K. Sahu, *Catal. Sci. Technol.* 1, 609 (2011).

40. H. T. Ren, S. Y. Jia, J. J. Zou, S. H. Wu, and X. Han, *Appl. Catal. B Environ.* 176-177, 53 (2015).

41. J. Sá, C. A. Agüera, S. Gross, and J. A. Anderson, *Appl. Catal. B Environ.* 85, 192 (2009).

42. J. A. Anderson, *Catal. Today* 175, 316 (2011).

43. I. Rossetti, A. Villa, C. Pirola, L. Prati, and G. Ramis, *RSC Adv.* 4, 28883 (2014).

44. I. Rossetti, *ISRN Chem. Eng.* 2012, 1 (2012).

45. I. Rossetti, A. Villa, M. Compagnoni, L. Prati, G. Ramis, C. Pirola, C. L. Bianchi, W. Wang, and D. Wang, *Catal. Sci. Technol.* 5, 4481 (2015).

46. W. Gao, R. Jin, J. Chen, X. Guan, H. Zeng, F. Zhang, and N. Guan, *Catal. Today* 90, 331 (2004).

47. J. Hirayama, H. Kondo, Y. K. Miura, R. Abe, and Y. Kamiya, *Catal. Commun.* 20, 99 (2012).

48. J. Hirayama and Y. Kamiya, *ACS Catal.* 4, 2207 (2014).

49. J. Hirayama, R. Abe, and Y. Kamiya, *Appl. Catal. B Environ.* 144, 721 (2014).

50. H. Kominami, A. Furusho, S. Murakami, and H. Inoue, *Catal. Letters* 76, 31 (2001).

51. H. Kominami, T. Nakaseko, Y. Shimada, A. Furusho, H. Inoue, S.-Y. Murakami, Y. Kera, and B. Ohtani, *Chem. Commun. (Camb).* 3, 2933 (2005).

52. N. Wehbe, M. Jaafar, C. Guillard, J. M. Herrmann, S. Miachon, E. Puzenat, and N. Guilhaume, *Appl. Catal. A Gen.* 368, 1 (2009).

53. M. Yamauchi, R. Abe, T. Tsukuda, K. Kato, and M. Takata, *J. Am. Chem. Soc.* 133, 1150 (2011).

54. L. Li, Z. Xu, F. Liu, Y. Shao, J. Wang, H. Wan, and S. Zheng, *J. Photochem. Photobiol. A Chem.* 212, 113 (2010).

55. O. S. G. P. Soares, M. F. R. Pereira, J. J. M. ??rf??o, J. L. Faria, and C. G. Silva, *Chem. Eng. J.* 251, 123 (2014).

56. L. Liu, X. Dong, and F. Yang, *2nd Int. Conf. Bioinforma. Biomed. Eng. iCBBE 2008* 3657 (2008).doi:10.1109/ICBBE.2008.416

57. D. D. B. Luiz, S. L. F. Andersen, C. Berger, H. J. José, and R. D. F. P. M. Moreira, *J. Photochem. Photobiol. A Chem.* 246, 36 (2012).

58. S. Rengaraj and X. Z. Li, *Chemosphere* 66, 930 (2007).

59. M. M. Mohamed, B. H. M. Asghar, and H. A. Muathen, *Catal. Commun.* 28, 58 (2012).

60. R. Jin, W. Gao, J. Chen, H. Zeng, F. Zhang, Z. Liu, and N. Guan, *J. Photochem.*

Photobiol. A Chem. 162, 585 (2004).

61. H. Kato and A. Kudo, *Phys. Chem. Chem. Phys.* 4, 2833 (2002).

62. R. M. Mohamed and E. S. Baeissa, *J. Ind. Eng. Chem.* 20, 1367 (2014).

63. Y. Wang, J. Yang, W. Gao, R. Cong, and T. Yang, *Mater. Lett.* 137, 99 (2014).

64. R. Wang, M. Yue, R. Cong, W. Gao, and T. Yang, *J. Alloys Compd.* 651, 731 (2015).

65. T. Mori, J. Suzuki, K. Fujimoto, M. Watanabe, and Y. Hasegawa, *J. Sol-Gel Sci. Technol.* 19, 505 (2000).

66. M. Oka, Y. Miseki, K. Saito, and A. Kudo, *Appl. Catal. B Environ.* 179, 407 (2015).

67. T. Sate, K. Sato, Y. Fujishiro, T. Yoshioka, and A. Okuwaki, *J. Chem. Tech. Biotechnol.* 67, 345 (1996).

68. S. Tawkaew, S. Yin, and T. Sato, *Int. J. Inorg. Mater.* 3, 855 (2001).

69. S. Tawkaew, Y. Fujishiro, S. Yin, and T. Sato, *Colloids Surfaces A Physicochem. Eng. Asp.* 179, 139 (2001).

70. D. de Bem Luiz, H. J. Josè, and R. de F. Peralta Muniz Moreira, *J. Chem. Technol. Biotechnol.* 90, 821 (2015).

71. K. Kobwittaya and S. Sirivithayapakorn, *J. Saudi Chem. Soc.* 18, 291 (2014).

72. D. J. Randall and T. K. N. Tsui, *Mar. Pollut. Bull.* 45, 17−23 (2002).

73. H. Mozzanega, J. M. Herrmann, and P. Pichat, *J. Phys. Chem.* 83, 2251 (1979).

74. A. Bravo, J. Garcia, X. Domènech, and J. Paral, *J. Chem. Res.* 376−377 (1993).

75. A. Wang, J. G. Edwards, and J. A. Davies, *Sol. Energy* 52, 459−466 (1994).

76. E. M. Bonsen, S. Schroeter, H. Jacobs, and J. A. C. Broekaert, *Chemosphere* 35, 1431−1445 (1997).

77. X. Zhu, S. R. Castleberry, M. A. Nanny, and E. C. Butler, *Environ. Sci. Technol.* 39, 3784−3791 (2005).

78. S. M. Murgia, A. Poletti, and R. Selvaggi, *Ann. Chim.* 95, 1−9 (2005).

79. X. Zhu, M. A. Nanny, and E. C. Butler, *J. Photochem. Photobiol., A* 185, 289−294 (2007).

80. K. M. Bark, H. S. Lee, W. H. Cho, and H. R. Park, *Bull. Korean Chem. Soc.* 29, 869−872 (2008).

81. S. Yamazoe, Y. Hitomi, T. Shishido, and T. Tanaka, *Appl. Catal. B Environ.* 82, 67−76 (2008).

82. M. Kaneko, H. Ueno, R. Saito, and J. Nemoto, *Catal. Lett.* 137, 156−162 (2010).

83. I. Mikami, S. Aoki, and Y. Miura, *Chem. Lett.* 39, 704 (2010).

84. J. Taguchi and T. Okuhara, *Appl. Catal. A Gen.* 194-195, 89 (2000).

85. J. Lee, H. Park, and W. Choi, *Environ. Sci. Technol.* 36, 5462 (2002).

86. H. Gerischer and Mauerer, *J. Electroanal. Chem.* 25, 421 (1970).

87. J. Nemoto, N. Gokan, H. Ueno, and M. Kaneko, *J. Photochem. Photobiol. A Chem.* 185, 295 (2007).

88. S. Shibuya, Y. Sekine, and I. Mikami, *Appl. Catal. A Gen.* 496, 73 (2015).

89. S. Shibuya, S. Aoki, Y. Sekine, and I. Mikami, *Appl. Catal. B Environ.* 138-139, 294 (2013).

90. H. Gerischer and A. Heller, *J. Phys. Chem.* 95, 5261 (1991).

91. K. Fuku, T. Kamegawa, K. Mori, and H. Yamashita, *Chem. Asian J.* 7, 1366 (2012).

92. H. Kominami, H. Nishimune, Y. Ohta, Y. Arakawa, and T. Inaba, *Appl. Catal. B Environ.* 111-112, 297 (2012).

93. Ł. Kowalczyk and M. I. Szynkowska, *Chem. Pap.* 66, 607 (2012).

94. M. Altomare and E. Selli, *Catal. Today* 209, 127 (2013).

95. M. V. Dozzi, L. Prati, P. Canton, and E. Selli, *Phys. Chem. Chem. Phys.* 11, 7171 (2009).

96. M. Altomare, G. L. Chiarello, A. Costa, M. Guarino, and E. Selli, *Chem. Eng. J.* 191, 394 (2012).

97. K. Obata, K. Kishishita, A. Okemoto, K. Taniya, Y. Ichihashi, and S. Nishiyama, *Appl. Catal. B Environ.* 160-161, 200 (2014).

98. M. Reli, N. Ambrožová, M. Šihor, L. Matějová, L. Čapek, L. Obalová, Z. Matěj, A. Kotarba, and K. Kočí, *Appl. Catal. B Environ.* 178, 108 (2015).

99. M. Reli, M. Edelmannová, M. Šihor, P. Praus, L. Svoboda, K. K. Mamulová, H. Otoupalíková, L. Čapek, A. Hospodková, L. Obalová, and K. Kočí, *Int. J. Hydrogen Energy* 40, 8530 (2015).

100. H. Yuzawa, T. Mori, H. Itoh, and H. Yoshida, *J. Phys. Chem. C* 116, 4126 (2012).

101. D. C. Hurum, A. G. Agrios, K. A. Gray, T. Rajh, and M. C. Thurnauer, *J. Phys. Chem. B* 107, 4545−4549 (2003).

102. B. Sun, A. V. Vorontsov, and P. G. Smirniotis, *Langmuir* 19, 3151−3156 (2003).

103. O. O. Prieto-Mahaney, N. Murakami, R. Abe, and B. Ohtani, *Chem. Lett.* 38, 238−239 (2009).

104. Y. Nosaka, K. Norimatsu, and H. Miyama, *Chem. Phys. Lett.* 106, 128−131 (1984).

105. S. Yamazoe, K. Teramura, Y. Hitomi, T. Shishido, and T. Tanaka, *J. Phys. Chem. C* 111, 14189−14197 (2007).

106. X. Zhu, S. R. Castleberry, M. A. Nanny, and E. C. Butler, *Environ. Sci. Technol.* 39, 3784 (2005).

107. M. Altomare, M. V. Dozzi, G. L. Chiarello, A. Di Paola, L. Palmisano, and E. Selli, *Catal. Today* 252, 184 (2015).

108. D. Sun, W. Sun, W. Yang, Q. Li, and J. K. Shang, *Chem. Eng. J.* 264, 728 (2015).

109. D. W. Bahnemann, M. Hilgendorff, and R. Memming, *J. Phys. Chem. B* 101, 4265 (1997).

110. D. C. Hurum, K. A. Gray, T. Rajh, and M. C. Thurnauer, *J. Phys. Chem. B* 109, 977 (2005).

111. X. Zhu, M. A. Nanny, and E. C. Butler, *J. Photochem. Photobiol. A Chem.* 185, 289 (2007).

112. G. V. Buxton, C. L. Greenstock, W. P. Helman, and A. B. Ross, *J. Phys. Chem. Ref. Data* 17, 514 (1988).

113. X. Zhu, M. A. Nanny, and E. C. Butler, *Water Res.* 42, 2736 (2008).

114. L. A. Pretzer, P. J. Carlson, and J. E. Boyd, *J. Photochem. Photobiol. A Chem.* 200, 246 (2008).

115. H. H. Ou, C. H. Liao, Y. H. Liou, J. H. Hong, and S. L. Lo, *Environ. Sci. Technol.* 42, 4507 (2008).

116. H. H. Ou, M. R. Hoffmann, C. H. Liao, J. H. Hong, and S. L. Lo, *Appl. Catal. B Environ.* 99, 74 (2010).

117. Y. Shavisi, S. Sharifnia, M. Zendehzaban, M. L. Mirghavami, and S. Kakehazar, *J. Ind. Eng. Chem.* 20, 2806 (2014).

118. J. Rongè, J. Bets, S. Pattanaik, T. Bosserez, S. Borellini, S. Pulinthanathu Sree, G. Decher, and J. A. Martens, *Catal. Today* 246, 28 (2015).

119. M. Kaneko, N. Katakura, C. Harada, Y. Takei, and M. Hoshino, *Chem. Commun. (Camb).* 3436 (2005).doi:10.1039/b502127h

120. S. Sun, W. Wang, L. Zhang, and M. Shang, *J. Phys. Chem. C* 113, 12826 (2009).

121. H. Wang, Y. Su, H. Zhao, H. Yu, S. Chen, Y. Zhang, and X. Quan, *Environ. Sci. Technol.* 48, 11984 (2014).

122. B. Xiao and S. Q. Liu, *Wuli Huaxue Xuebao/ Acta Phys. - Chim. Sin.* 30, 1697 (2014).

123. L. Zhang, W. Wang, and S. Sun, *Chinese Sci. Bull.* 59, 2181 (2014).

124. Y. Zhou, B. Xiao, S. Q. Liu, Z. Meng, Z. G. Chen, C. Y. Zou, C. B. Liu, F. Chen, and X. Zhou, *Chem. Eng. J.* 283, 266 (2016).

125. M. Kaneko, H. Ueno, R. Saito, and J. Nemoto, *Catal. Letters* 137, 156 (2010).

GRAPHICAL ABSTRACT
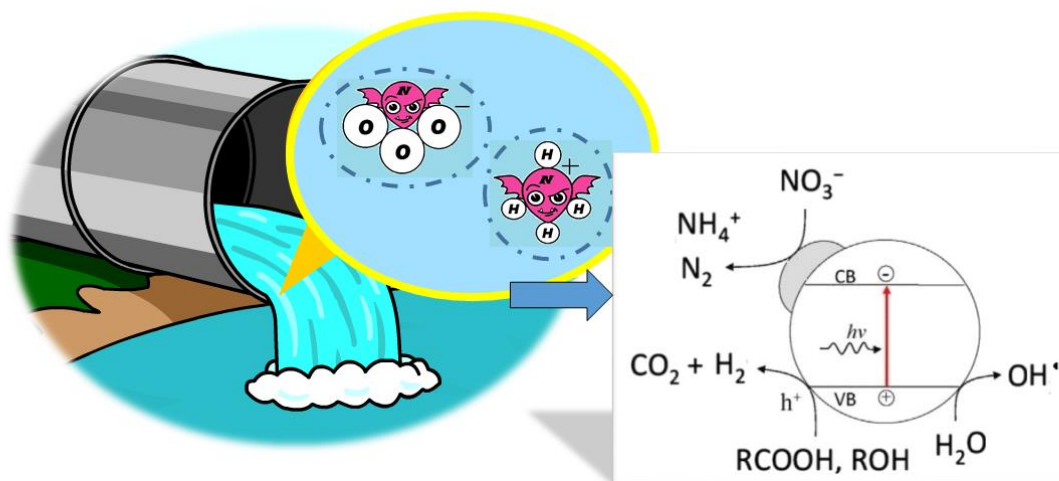
Ammonia, nitrites and nitrates are harmful contaminants for drinking water, inducing acute and/or chronic diseases, especially affecting infants and children; they contribute to eutrophication, or possibly contaminate ground water.

In the present paper, we review existing or innovative processes, mainly based on photocatalytic steps for the abatement of inorganic N-containing compounds from waste waters and for drinking water treatment, focusing on selectivity towards innocuous N_2.